Sibgha TAHIR

QUANTITATIVE PCR ANALYSIS OF GENE EXPRESSION IN ENDOTHELIAL CELLS EXPOSED TO SHEAR STRESS AT BRANCHING POINTS IN ARTERIES LEADING TO ATHEROSCLEROSIS

M.S.
2013

FATIH UNIVERSITY

The Graduate School of Sciences and Engineering

Master of Science in
Genetics and Bioengineering

QUANTITATIVE PCR ANALYSIS OF GENE EXPRESSION IN ENDOTHELIAL CELLS EXPOSED TO SHEAR STRESS AT BRANCHING POINTS IN ARTERIES LEADING TO ATHEROSCLEROSIS

by

Sibgha TAHIR

June 2013

QUANTITATIVE PCR ANALYSIS OF GENE EXPRESSION IN ENDOTHELIAL CELLS EXPOSED TO SHEAR STRESS AT BRANCHING POINTS IN ARTERIES LEADING TO ATHEROSCLEROSIS

by

Sibgha TAHIR

A thesis submitted to

The Graduate School of Sciences and Engineering

of

Fatih University

in partial fulfillment of the requirements for the degree of

Master of Science

in

Genetics and Bioengineering

June, 2013
Istanbul, Turkey

APPROVAL PAGE

This is to certify that I have read this thesis written by Sibgha TAHIR and that in my opinion it is fully adequate, in scope and quality, as a thesis for the degree of Master of Science in Genetics and Bioengineering.

_____

Assoc. Prof. Dr. Nurullah ARSLAN
Thesis Supervisor

_____

Assistant Prof. Dr. Fahri AKBAŞ
Co-Supervisor

I certify that this thesis satisfies all the requirements as a thesis for the degree of Master of Science in Genetics and Bioengineering.

_____

Prof. Dr. Halil Rıdvan ÖZ
Head of Department

Examining Committee Members

Assoc. Prof. Dr. Nurullah ARSLAN _____

Assist. Prof. Dr. Fahri AKBAŞ _____

Assoc. Prof. Dr. Mustafa Fatih ABASIYANIK _____

Assoc. Prof. Dr. Barık SALİH _____

Assist. Prof. Dr. Haşim Özgür TABAKOĞLU _____

It is approved that this thesis has been written in compliance with the formatting rules laid down by the Graduate School of Sciences and Engineering.

_____

Assoc. Prof. Dr. Nurullah ARSLAN
Director

June, 2013

QUANTITATIVE PCR ANALYSIS OF GENE EXPRESSION IN ENDOTHELIAL CELLS EXPOSED TO SHEAR STRESS AT BRANCHING POINTS IN ARTERIES LEADING TO ATHEROSCLEROSIS

Sibgha TAHIR

M.S. Thesis – Genetics and Bioengineering
June 2013

Thesis Supervisor: Assoc. Prof. Dr. Nurullah ARSLAN

Co-Supervisor: Assist. Prof. Dr. Fahri AKBAŞ

ABSTRACT

Atherosclerosis being the most common cause of cardiovascular disease not only depends on risk factors like smoking, hypertension or high cholesterol level but also on the geometry of arteries. It is preferentially located at the branched and curved regions rather than the straight regions of arteries due to the variation in shear stress depending on the pattern of flow. In straight regions of arteries the flow is laminar and exerts high shear stress (HSS) while in branched regions, the flow is disturbed and exerts low shear stress (LSS). ECs lining the inner membrane of arteries sense and transduce blood flow associated shear stress, resulting in expression of various genes that lead to atherosclerosis. In our study, we have analyzed the morphological changes as well as variation in gene expression of HUVECs exposed to shear stress in a newly designed branched kit of parallel plate flow chamber. After dynamic simulation, a flow rate of 50 ml/min was applied over cells. Firstly, the cells were compared in their morphology under laminar and disturbed flow region of branched kit. In laminar flow region HUVECs tend to elongate in the direction of flow whereas in disturbed flow region they showed polygonal shape. Secondly, HUVECs were collected for qPCR analysis. Gene expression of cells under both laminar and disturbed flow region was analyzed. Ct values obtained by real time PCR were then exported for ΔΔCt analysis by which 9 miRNAs were found to be downregulated and 13 miRNAs upregulated in disturbed flow region as compared to laminar flow region. The affected miRNAs were searched in miRNA database for their target prediction and correlation with atherosclerosis. All the affected miRNAs except hsa-miR-96 were involved in regulating CVD. The results

demonstrated that in disturbed flow region, LSS causes the variation in expression of miRNAs that directly regulate the progression of atherosclerosis and other heart diseases.

Keywords: Atherosclerosis, ECs, HUVECs, Shear stress, Laminar flow, Disturbed flow, Branched kit parallel plate flow chamber, miRNA, qPCR, Ct and miRNA database.

ATARDAMAR DALLANMA BÖLGELERİNDE ATEROSKLEROSİSE SEBEBİYET VEREN KAYMA GERİLMELERİNE MARUZ ENDOTEL HÜCRELERİNDE GEN EKSPRESYONUN KANTİTATİF PCR METODU İLE ANALİZİ

Sibgha TAHIR

Yüksek Lisans Tezi – Genetik ve Biyomühendisliği
Haziran 2013

Tez Danışmanı: Assoc. Prof. Dr. Nurullah ARSLAN

Eş Danışman: Assist. Prof. Dr. Fahri AKBAŞ

ÖZ

Kardiyovasküler hastalıkların en önemli nedeni olan aterosklerosis sadece sigara kullanımı, hipertansiyon yada yüksek kolesterol gibi risk faktörlerine değil aynı zamanda atardamarların geometrisinede bağlıdır. Akışın geometric şekline bağlı olarak değişen kayma gerilmeleriyle atardamarın düzgün kısımlarında değil daha çok dallanan ve eğimli bölgelerinde yeralır. Düzgün bölgelerde akış laminar akıştır ve yüksek kayma gerilmelerine neden olur, dallanan bölgelerde ise akış düzensiz akış ve düşük kayma gerilmelerine neden olur. Atardamarların iç yüzeyini oluşturan Endotel hücreleri kan akışını algılar ve kayma gerilmesini dönüştürür buda aterosklerosise neden olan değişik genlerin eksprese olmasına neden olur. Çalışmamızda tarafımızdan imal edilen bir akış kitinin içerisinden geçen akışın HUVEC hücreleri üzerine uyguladığı kayma gerilmesinin etkisini morfolojik ve genetik açıdan analiz ettik. Dinamik benzeşim metodu kullanılarak hücreler üzerine 50 ml/min akış debisi uygulanmıştır. İlk olarak hücrelerin morfolojisi dallanma bölgesinde laminar ve sürekli olmayan akış şartlarında karşılaştırılmıştır. Laminer akışta hücrelerin akışın yönünde uzadığı gözlemlenmiştir. Sürekli olmayan akış altında hücreler poligonal bir şekil almışlardır. İkinci olarak qPCR analizi için HUVEC ler toplanmıştır. Laminer ve sürekli olmayan akış şartlarında gen ekspresyonuna bakılmıştır. Gerçek zamanlı PCR yoluyla elde edilen Ct değerleri, ΔΔCt analizi ile sürekli olmayan akış bölgesinde 9 miRNAs azaldığı 13 miRNAs ise çoğaldığı gözlemlenmiştir. Etkilenen miRNA lerin miRNA data dosyasından atherosclerosis ile korelasyonuna bakılmıştır. hsa-miR-96 hariç tüm etkilenen miRNAs CVD regülasyonunda bulunmuşlardır. Sonuçlar sürekli olmayan akış bölgesinde düşük kayma

gerilmesinin miRNA ekspresyonuna neden olduğunu buda atherosclerosis ve diğer kalp problemlerine neden olabileceğini göstermiştir.

Anahtar Kelimeler: Aterosklerosis, Endotel hücreleri, HUVEC, Kayma gerilmesi, Laminer akış, Sürekli olmayan akış, parallel akış kiti, miRNA, qPCR.

To My Parents

ACKNOWLEDGEMENTS

All praise is to Allah Who has enabled me enough to put some successful effort in the fulfillment of this research work. First of all support and prayers of my Parents and affectionate co-operation of my siblings made it possible for me to study and work abroad.

I would like to pay my deepest gratitude to my respectable supervisor Assoc. Prof. Dr. Nurullah ARSLAN who has always been a source of knowledge and inspiration for me. He has been quite tolerant and supportive towards my work in lab. His affection and firmness both stimulated me to work hard. I am thankful for the knowledge he has given to me. I pray to Allah that He may bless him always. Ameen!

I express my sincere appreciation and gratitude to my co-supervisor Dr. Fahri AKBAŞ for his valuable suggestions and guidance throughout the research. Because of his knowledgeable discussions and experience of scientific research it was possible to analyze the results of this fruitful research.

Special thanks to Fatih University for supporting my thesis with Project No: P50091101_B (1580). The facilities provided by Fatih University in particular from mechanical workshop by Mr. Ertan AKÇA to devise new flow kit is appreciable without the provision of which it would have been difficult to carry out my experiments.

Last but not the least I would like to regard all my teachers because of whom I had been able to do something worthwhile, especially Dr Barık SALIH who has groomed me as a scientist from a mere superficial learner.

TABLE OF CONTENTS

LIST OF TABLES

TABLE

LIST OF FIGURES

FIGURE

LIST OF SYMBOLS AND ABBREVIATIONS

SYMBOL/ABBREVIATION	
BAEC	Bovine aortic endothelial cell
CVD	Cardiovascular Disease
Ct	Cycle of threshold
DMEM	Dulbecco's Modified Eagle Medium
ECs	Endothelial Cells
FBS	Fetal Bovine Serum
HAEC	Human aortic endothelial cell
HSS	High Shear Stress
HUVECs	Human Umbilical Vein Endothelial Cells
ICAM	Intercellular cell adhesion molecule
LDL	Low Density Lipoprotein
LSS	Low Shear Stress
MCP1	Monocyte Chemotactic Protein-1
miRNA	Micro RNA
NO	Nitric oxide
PBS	Phosphate Buffer Saline
PCR	Polymerase Chain Reaction
PDGF	Platelet derived growth factor
Re	Reynolds number
ROS	Reactive oxygen specie
SMC	Smooth muscle cell
UTR	Untranslated region
VCAM	Vascular cell adhesion molecule
Q	Flow rate
μ	Viscosity

ρ	Density
U	Velocity
D	Diameter

CHAPTER 1

INTRODUCTION

The abnormality in function of cardiovascular system is given a name in literature called cardiovascular disease (CVD). It involves the heart and blood vessels that are mostly affected by atherosclerosis and hypertension. CVD is a leading cause of death in developed countries where the mortality rate due to this disease is 49 % of all deaths in Europe and 38 % in U.S [1].

1.1 ATHEROSCLEROSIS

Atherosclerosis is an inflammatory disease in which an artery wall thickens by formation of plaque due to accumulation of biochemicals like cholesterol, triglyceride, calcium, fibrin, collagen, low density lipoproteins (LDL) and the cells like macrophages, white blood cells, T cells, smooth muscle cells and cell debris that reduce the lumen, sometimes completely blocking the blood flow [2]. Due to blockage of blood flow, the tissues deprived of oxygen and nutrients start to die which is known as ischemia. It can lead to fatal consequences, even death by myocardial infarction and heart congestion.

The low density lipoprotein (LDL) particle acts as a major transporter of cholesterol in the body and is a great risk factor of causing atherosclerosis. The atherosclerotic plaque contains a lipid rich core filled with cholesterol, fatty acids and necrotic tissues which is covered by a cell cap. LDL is responsible for the major accumulation of cholesterol in this plaque. LDL has an ability to attach to endothelium.

surface by lipoprotein lipase and heparin sulphate proteoglycans which assist its uptake into sub endothelial space. Macrophages engulf cholesterol and attach to vascular cell adhesion molecule (VCAM) and intercellular cell adhesion molecule (ICAM) present on endothelial surface and permeate into intima where they differentiate into foam cells. Eventually foam cells break up and release the cholesterol for lipid rich atherosclerotic core [3].

1.2 HEALTHY ARTERIAL WALL

The healthy arterial wall is composed of three layers called tunicae which are present in all blood vessels. These three layers are named as: tunica intima, tunica media and tunica adventitia. The intima is a thin single layer of endothelial cells that resides on ~80 nm basal lamina of type IV collagen. They act as semi permeable membrane that allows the nutrients and chemical signals from bloodstream to reach the cells forming vessel wall. The intima is separated from the media by a fine sheet of elastin called internal elastic lamina [4].

Smooth muscle cells (SMC) primarily form the middle layer, tunica media, of arterial wall that are embedded in an extracellular matrix of type I elastin, type III collagen and proteoglycans. The arteries are characterized into elastic and muscular arteries depending on the arrangement of SMC in tunica media. The elastic arteries are large in diameter and include vessels close to heart that are aorta, the main pulmonary artery, the common carotid and iliac arteries. Their important characteristic is a sublayer of SMC and thin elastic laminae arranged like a sandwich which is called lamellar unit. The elastic arteries consist of concentric ring like structures in tunica media that range from 40 to 70 in aorta, and they are tied together by radially oriented collagen. SMC form a single thick ring in tunica media of muscular arteries which are embedded in a loose matrix of connective tissue. They are arranged in a concentric layer of cells which may vary from 25 to 40 in large vessels like femoral artery.

The outermost layer of artery wall, tunica adventitia, is composed of dense network of type I collagen with scattered fibroblasts, elastin and nerves. The nerves in adventitia are responsible for the innervation of SMC in outer media through the

diffusion of neurotransmitters. Fibroblasts play a role in the synthesis of collagen particularly types I, thus regulating the connective tissue. Adventitia is accountable for preventing rupture of the vessel by gradually straightening its fibers if there is an acute increase in pressure [4]. The structure of an artery wall is described in detail in Figure 1.1.

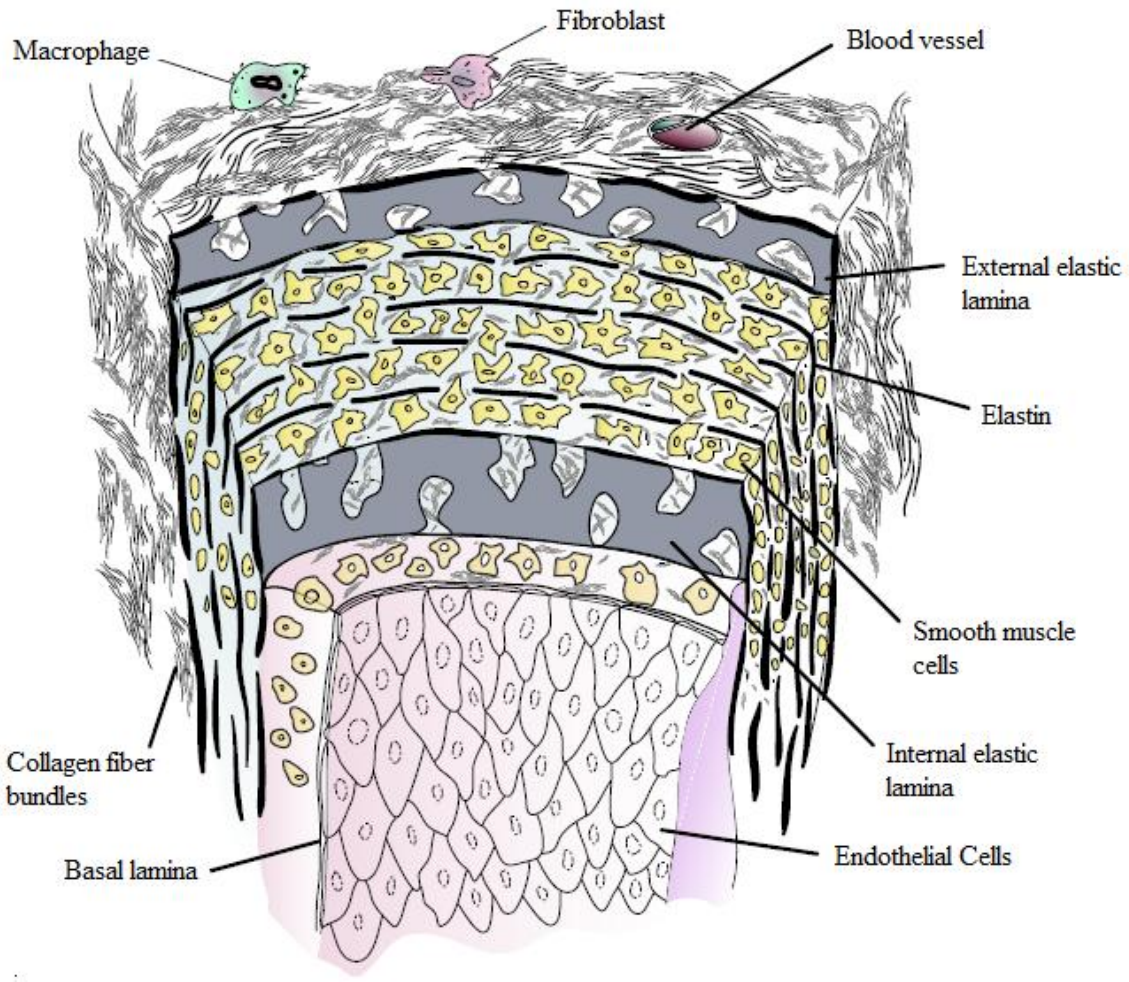

Figure 1.1 Structure of a healthy artery [5].

1.3 PROGRESSION OF ATHEROSCLEROSIS

The earliest changes that precede atherosclerosis are observed in endothelium of arteries which include increased endothelial permeability for lipoproteins and various

plasma constituents. This increased endothelial permeability is mediated by number of factors that include nitric oxide, angiotensin II, prostacyclin, endothelin and platelet derived growth factor. The inability of endothelium to respond to nitric oxide may be the first abnormality in disease progression [3]. Figure 1.2 is showing the initial stage of disease progression in which endothelial permeability for leukocytes and plasma contents is increased [6].

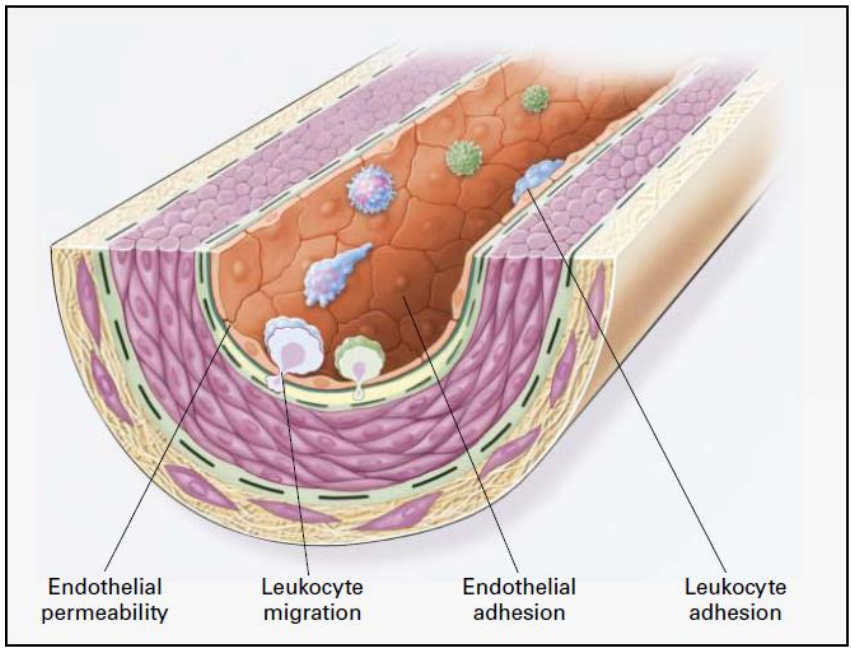

Figure 1.2 Initial stage of disease progression [6].

Atherosclerosis begins with the formation of fatty plaques by trapping of lipoproteins at the lesion prone sites due to an imbalance of LDL concentration between plasma and tissue. This leads to accumulation of lipids in extracellular matrix of basal zone of intima. The pathology of lipid accumulation causes increase in leukocytes that adhere to endothelial surface through specific adhesion molecules expressed on endothelial surface. The up-regulation of these adhesion molecules that include E-selectin, P-selectin, intercellular adhesion molecule 1 and vascular adhesion molecule is mediated by monocyte, chemotactic protein 1, macrophage colony stimulating factor, interleukin-8, platelet derived growth factor and osteopontin. At the start of

inflammatory response leukocytes arrive at the site of dysfunction as a result of which monocytes enter the artery wall where they differentiate into macrophages. Macrophages subsequently transform into foam cells by engulfing trapped lipoproteins. Many of these foam cells then become activated by expressing a variety of additional factors that provide favourable biochemical environment for atherogenic process and disease progression. Figure 1.3 describes the disease progression from the accumulation of LDL that migrates through intima of endothelium at the left side to the thickening of intima at the right side [7].

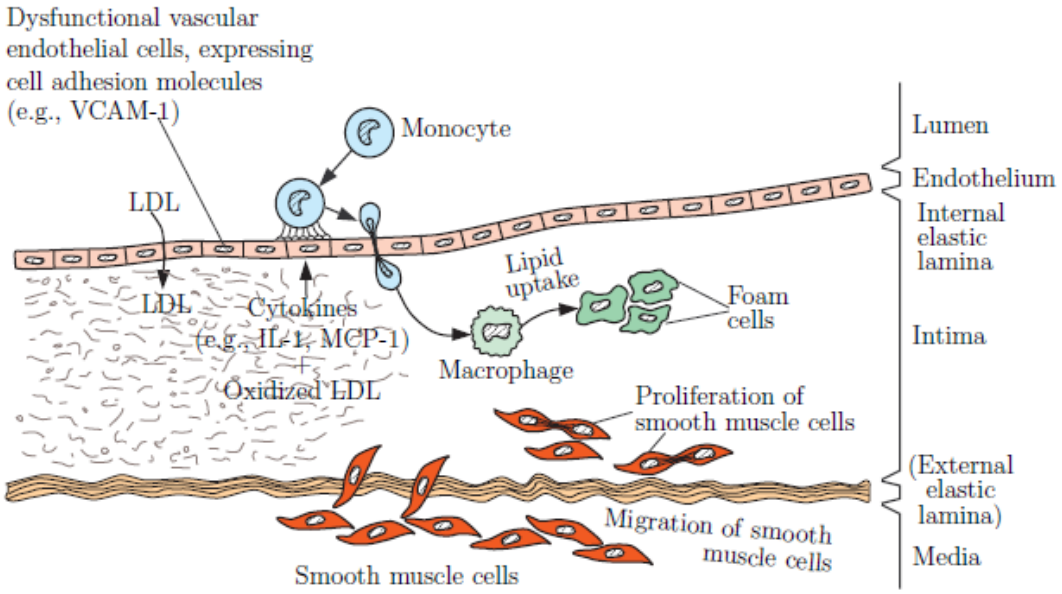

Figure 1.3 Progression of atherosclerosis [7].

Atherogenic plaque initially consists of foam cells together with T-lymphocytes. Afterwards the plaque is joined by smooth muscle cells due to their migration from tunica media which is stimulated by fibroblast growth factor 2, transforming growth factor *b* and platelet-derived growth factor. Figure 1.4 explains the fatty streak formation in atherosclerosis due to accumulation of foam cells, immune cells and various other plasma contents.

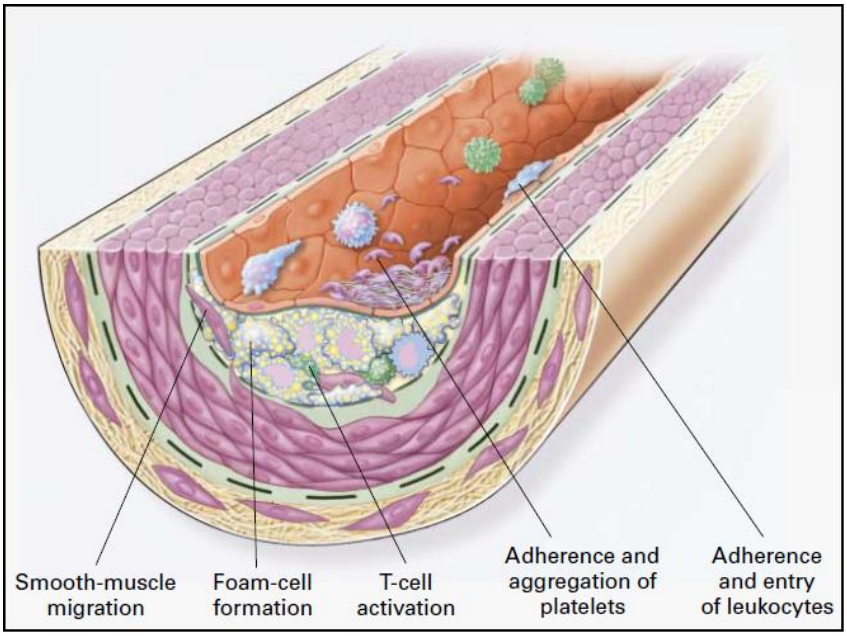

Figure 1.4 Thickening of arteries in atherosclerosis [6].

Vascular stiffness is an early manifestation of atherosclerosis that occurs due to increase in epicardial and pericardial adipose tissue. Increased adipose tissue level being the cause of obesity thus also has an effect on coronary atherosclerosis [8].

1.1 ATHEROSCLEROSIS VS. HEMODYNAMICS

The progression of atherosclerosis and other cardiovascular diseases have been linked to hemodynamics also. Atherosclerosis is commonly observed at the sites of disturbed flow patterns preferably the junctions and branches of arterial system like coronary arteries and carotid bifurcation. The branches, bifurcations and curvatures pose alteration in the pattern of blood flow that includes decreased shear stress and increased turbulence [9]. There are number of evidences that show the dependence of physiological activity of endothelium on variables such as stress and strain within in the tissue, because they cause atherosclerotic plaques to be developed in curved regions of the arteries rather than straight regions [10, 11]. These stresses act on or within the arterial wall where they are responsible for the expression of specific adhesion

molecules on endothelium surface for adherence, migration and accumulation of monocytes and T lymphocytes.

It is now appreciated that the normal function of the single-cell-thick endothelial lining of the circulatory system is essential for vascular homeostasis in health and that its dysfunction plays a significant role in many vascular diseases. The idea of shear stress effect to cause atherosclerosis prompts us to carry out our experiments on endothelial cells with shear stress over them by applying flow. Further we aimed to analyze the difference in gene expression of cells that were under the influence of disturbed flow, laminar flow and static conditions in order to unravel the genes which are mostly affected by disturbed flow pattern.

CHAPTER 2

LITERATURE REVIEW

The first lesions of atherosclerosis were observed preferentially at the arterial bifurcations and curvatures where the flow is disturbed, suggesting the possible role of hemodynamic forces in endothelial dysfunction. Figure 2.1 shows the likely regions of arterial system where there are more chances of atherosclerosis localization. It is apparent that the branches and curvatures are more vulnerable to disease.

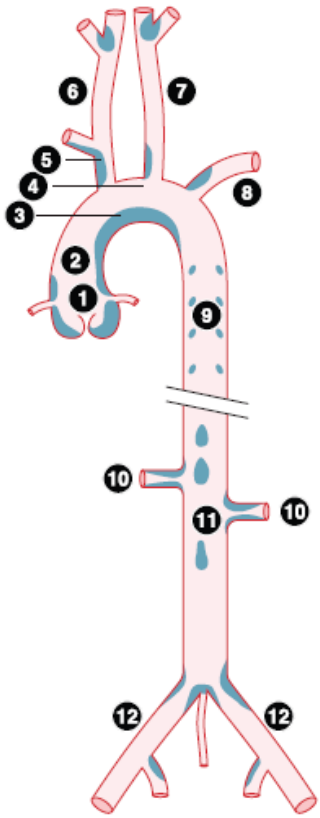

Figure 2.1 Localization of atherosclerosis in arterial system [12].

In a recent study, localization of complex plaques was found to be at the inner curvature of aortic arch and descending aorta [13]. Distal regions of coronary arteries are inhabited by advanced coronary plaques which are exposed to low shear stress and they exhibit a stable plaque phenotype [14]. Vascular endothelial cells present in tunica intima of blood vessel are in direct contact with blood flow and its associated hemodynamic forces. They control various homeostatic functions by responding to chemical and mechanical stimuli [15-20]. Endothelial cells not only serve as selective permeable membrane for plasma contents but also influence vascular modelling by producing growth promoting and inhibiting substances, by expressing cell adhesion molecules on their surface and by secretion of chemokines and cytokines. They also regulate contraction of vascular smooth muscle cells by maintaining balance between vasodilators and vasoconstrictors [18]. Endothelial dysfunction can cause vascular disorders resulting from atherosclerosis, thrombosis and other complications [21-24].

2.1 HEMODYNAMIC FORCES AND ENDOTHELIAL DYSFUNCTION

Blood vessels are under the constant influence of variety of hemodynamic forces that include fluid shear stress, hydrostatic pressure and cyclic stretch which are induced by the pulsatile nature of blood flow. Figure 2.2 explains the different forces acting upon the endothelium.

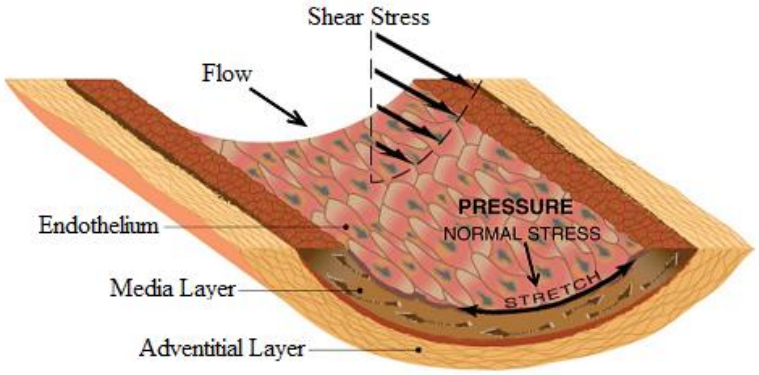

Figure 2.2 Hemodynamic forces acting on endothelium [24].

Some of the hemodynamic forces are essential for physiological functioning of endothelial cells under normal conditions while other forces contribute to vascular pathologies like atherosclerosis by endothelial dysfunction as a result of modulating cell signalling and gene expression [25-28]. At the branched region of arteries where atherosclerosis is preferentially observed, the flow is disturbed that comprises recirculation eddies [29]. ECs bear most of the shear stress originating from the blood flow being part of the frictional forces that act parallel to blood vessel luminal surface [30]. Researchers have shown that in humans the magnitude of shear stress in arteries ranges from 10 to 70 dyn/cm^2 [31]. As endothelium is primarily controlling the contractility of vascular SMC by the release of vasodilators (nitric oxide (NO) and prostacyclin) and vasoconstrictors (thromboxane A_2, reactive oxygen species (ROS), endothelin and angiotensin II), so if there is any imbalance between them it can lead to early stages of atherosclerosis [32]. According to many studies decrease in bioavailability of NO by inactivation of superoxide anion leads to atherosclerosis [33-35]. There are many evidences that hemodynamic forces affect the structure and function of ECs by modulating the expression of relevant genes [36-39]. In straight part of arterial system the flow is laminar with high shear stress of 10-70 dyn/cm^2 [40]. Vascular ECs which are under high shear stress in laminar regions constantly release NO which maintains the contractility of underlying SMC [41]. While in the complex geometries that include branch points and curvatures, there is a disturbance in flow pattern that lead to less net forward flow and low shear stress (<4 dyn/cm^2). In such complex regions flow alters the NO production capability of endothelium hence inducing endothelial dysfunction [42]. According to different researches the endothelium dependent vasodilation of SMC is defective at branched regions of coronary arteries [42-43]. So hemodynamic forces are involved in altering the normal function of ECs by variation of shear stress, which can trigger expression of various genes involved in atherosclerotic progression.

2.2 EFFECTS OF DISTURBED FLOW ON VASCULAR ENDOTHELIUM *IN VITRO*

A variety of *in vitro* models have been designed in the recent past in order to apply shear stress on ECs, mimicking the *in vivo* environment, and then analyzing the

response mechanisms. These models include parallel plate flow chamber, cone and plate viscometer, parallel disk viscometer, orbital shaker and tubular capillary tube [44-48]. Figure 2.3 shows the configurations of these *in vitro* models.

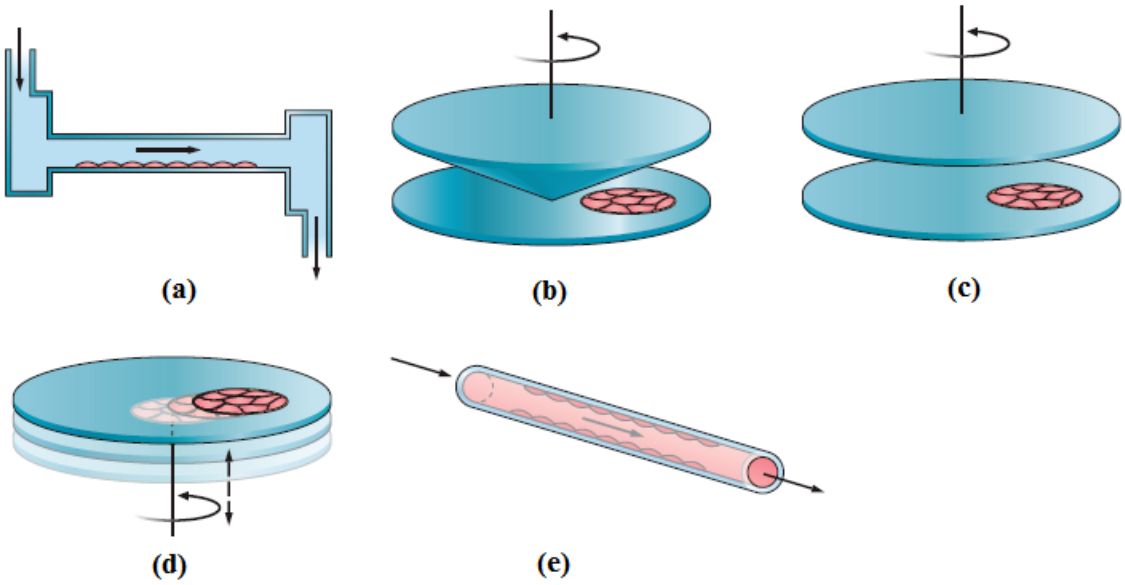

Figure 2.3 Configurations of *in vitro* models for applying shear stress on ECs. (a).parallel plate flow chamber, (b) cone and plate viscometer, (c) parallel disk viscometer, (d) orbital shaker and (e) tubular capillary tube [24].

Parallel disk viscometer and orbital shaker cannot provide uniform shear stress over monolayer ECs and tubular capillary tube do not yield sufficient amount of ECs for bioassays. The systems based on parallel plate flow chamber and cone and plate viscometer have the ability to provide uniform shear stress over ECs monolayer as well as yield sufficient amount of cells for bioassays, that's why these models have been used widely for studying ECs responses to shear stress. Several *in vitro* models have been designed on the basis of parallel plate flow chamber and cone and plate viscometer to mimic the complex flow patterns in arterial system. Different studies involved parallel plate flow chamber in which disturbed flow was created by placing a step near the inlet by silicone gaskets. ECs when subjected to flow in a channel showed the response against both laminar and disturbed flows.

An *in vitro* study on porcine left common carotid artery has shown that in response to bradykinin there was a low shear stress in curved regions that decrease the expression of endothelial NO synthase gene. This leads to decreased vasodilation as compared to regions of laminar shear stress. This study suggests that hemodynamic flow patterns impair the function of ECs in carotid arteries [44]. It was further studied that the endothelial dysfunction caused by decreased shear stress and blood flow can be reversed by increasing the level of shear stress with the help of physical exercise [45].

2.3 EFFECTS OF DISTURBED FLOW ON VASCULAR ENDOTHELIUM *IN VIVO*

In vivo studies have shown that the variation in shear stress rather than the absolute value of shear stress is responsible for maintaining vascular homeostasis [46]. There has been limited number of *in vivo* studies on ECs response to shear stress and disturbed flow due to insufficient animal models that can generate disturbed flow patterns. Several animal models have been created in order to study the ECs response to disturbed flow. These models were established by:

1. Creating arteriovenous fistula by using carotid arteries [47].
2. Ligation of carotid arteries to increase shear stress [48].
3. Transposing vein graft into arterial system to increase shear stress [49].

Disturbed flow pattern and associated low shear stress was created in arteries by the most common strategy of introducing stenosis in a segment of vessel as done in rabbits and rats [50]. Using this strategy it was found that ECs tend to elongate in the direction of flow but upstream of stenotic region where the flow was laminar and in the region involving flow separation and low velocity recirculation, the ECs were predominantly rounded. Similar results were reported by couple of other researches [51, 52].

Regarding gene analysis a study has been done by a research group who analyzed that the expression of *tie1* promoter is enhanced in the arterial tree where there is

curvatures and branch point i.e. the regions of disturbed flow [53]. *In vivo* studies have shown that ECs show increase in mitotic division, lipid uptake and monocyte adhesion in the region of disturbed flow [54]. Due to change in morphology of ECs there is an increase in expression of number of genes that include ICAM-1, VCAM-1, E-selectin, PDGFs, Egr-1 and many more [55].

Many *in vivo* studies have proved that HSS decrease the expression of proatherogenic genes and increase the expression of atheroprotective genes whereas LSS performs the opposite function. One of the very important genetic investigations was done on ECs in which a shear stress of 12 dyn/cm^2 was applied on human aortic ECs (HAEC). The HSS effect was then analyzed on more than 1000 genes especially related to cell proliferation, remodelling, cytoskeleton, signal transduction and inflammation by using microarray chip. Out of these 1000 genes, 125 were significantly affected. Proatherogenic genes including 10 MYD88, CD30 ligand were decreased and atheroprotective genes like *tie2* and *flk1* were upregulated that play role in EC survival [56].

Expression of tumor suppressor gene p53, the growth arrest proteins GADD45 and p21cip1 was increased in bovine aortic endothelial cells (BAEC) when exposed to a shear stress of 12 dyn/cm^2 [57]. NO is atheroprotective due to its role in vasodilation, anti-thrombotic and anti-inflammatory processes. It is synthesized by endothelial NO synthase (eNOS). According to various studies, expression of eNOS is upregulated by HSS or laminar flow and downregulated by LSS or disturbed flow [58-61].

2.4 EFFECTS OF SHEAR STRESS ON miRNA

MicroRNA (miRNA) is a short RNA strand comprising 21-25 nucleotides. miRNA plays important role in post-transcriptional regulation of mRNA. Functional miRNA binds to untranslated regions (UTRs) of target mRNAs by partial complementarity. This event prevents mRNA translation by degradation of mRNA or repression of translation without mRNA cleavage.

Shear stress is responsible for regulating gene expression via many ways and one of them is by regulating miRNA expression. Shear stress affects the expression of

miRNA by increasing or decreasing its level which in response can increase or decrease the expression of target mRNA. According to one research, when HUVECs were exposed to laminar shear stress of 12 dyn/cm^2 they showed a change in expression of 61 significant miRNA. 35 miRNAs were upregulated and 26 downregulated as result of exposure to laminar flow [62].

In our research work we have focused on variation in gene expression in HUVECs exposed to shear stress mostly in disturbed flow regions of arteries. miRNA expression and their target genes were analyzed in order to establish their role in causing atherosclerosis majorly in curvatures and branched regions.

CHAPTER 3

MATERIALS AND METHODS

3.4 MATERIALS

For the accomplishment of our experiment, to analyze the effect of shear stress on the differential gene expression of endothelial cells (ECs), the equipments utilized are listed in the Table 3.1.

Table 3.1 List of equipments.

Sr. No.	EQUIPMENTS	COMPANY
1	Laminar Flow	ESCO
2	CO_2 Incubator	THERMO SCIENTIFIC
3	Inverted Microscope	LEICA
4	Centrifuge 15ml TC	NÜVE
5	Refrigerator	BOSCH
6	-80^{o}C Freezer	DAIHAN
7	Autoclave	ALP
8	Distilled Water Machine	MILLIPORE
9	Sensitive Balance	PRECISA
10	Leica Application Suite	LEICA SOFTWARE
11	Microscope Camera	CANON
12	Sterile Serologic Pipettes 2 ml, 5 ml, 10 ml, 25 ml	GREINER BIO-ONE
13	Tygon Hoses 15 mm	MASTERFLEX
14	High Performance Pump Model 77250-62	MASTERFLEX

Table 3.1 (Cont.)

Sr. No.	EQUIPMENTS	COMPANY
15	Parallel Plate Flow Chamber	FATIH UNIVERSITY MECHANICAL WORKSHOP
16	Water Bath	THERMO SCIENTIFIC
17	Cell Culture Dishes 60mm	GREINER BIO-ONE
18	25-75 mm Glass Slide	LOGITECH
19	MiniCentrifuge (eppendorf)	THERMO SCIENTIFIC
20	Nanodrop 2000 Spectrophotometer	THERMO SCIENTIFIC
21	Micropipettes	THERMO SCIENTIFIC
22	Micropipette Tips	GREINER BIO-ONE
23	PCR Tubes(0.2 ml)	GREINER BIO-ONE

The materials used for culturing of ECs, their seeding and carrying out gene analysis are given in Table 3.2.

Table 3.2 List of materials.

Sr. No.	Materials	Company
1	HUVECs	BIOLOGY LAB
2	DMEM with L-glutamine	BIOCHROM
3	FBS	BIOCHROM
4	Penicillin/Streptomycin	INVITROGEN
5	PBS	BIOCHROM
6	Trypsin 0.25% EDTA	INVITROGEN
7	Gelatin Powder	MERCK
8	RNA Isolation Kit	ROCHE
9	cDNA Synthesis Kit	ROCHE
10	miScript RNA Kit	QIAGEN
11	PCR Kit	SYBR GREEN
12	PSP (5μm) Polyamid Seeding Particles	DANTEC DYNAMICS

3.1.1 Branched Kit of Parallel Plate Flow Chamber

The most important equipment utilized to study the effect of flow over ECs was the parallel plate flow chamber. Parallel plate flow chamber is an *in vitro* model to study the effect of shear stress on various cell types. With the help of this device it is possible to study the effect of constant shear stress on HUVECs for a defined period of time. The cells can be grown as well under flow conditions and can be observed under inverted microscope. For the manufacturing of new design of parallel plate flow kit with a branched plate inside, certain parameters were kept in observation. Firstly, the chamber should be autoclavable and resist high temperature of 121 ^{o}C so that it can be sterilized for HUVECs growth. Secondly, it should be resistant to certain chemicals like ethanol etc that can affect the chamber transparency when being exposed. Thirdly, it should transmit light to be better observed under inverted microscope for continuously observing HUVECs. And lastly, for our required experiment the chamber should have a branched plate to mimic the branched region and curvature of arteries. So, we designed a novel model by keeping in consideration all these requirements from aluminum and glass. The new model is described in detail in Figure 3.1.

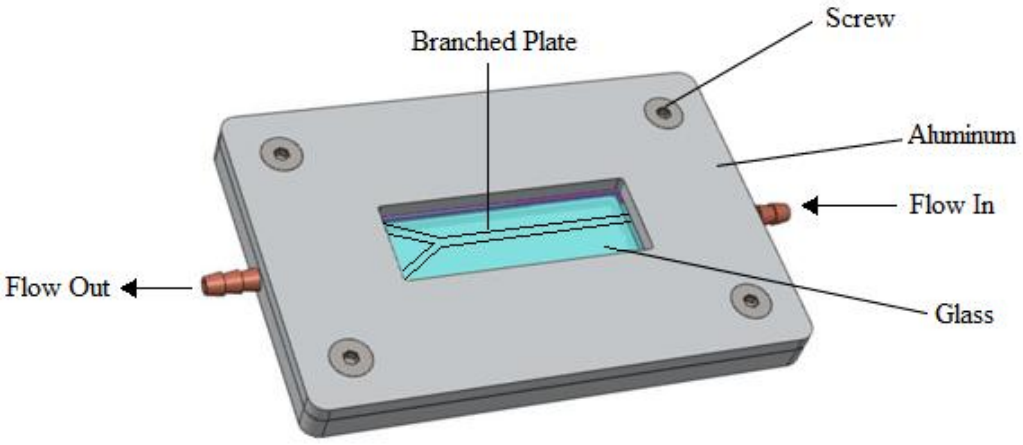

(a)

Figure 3.1 Detailed description of branched kit parallel plate flow chamber. (a) Schematic diagram, (b) Novel modification by changing the linear plate with branched one, (c) Components of chamber, (d) Realistic model.

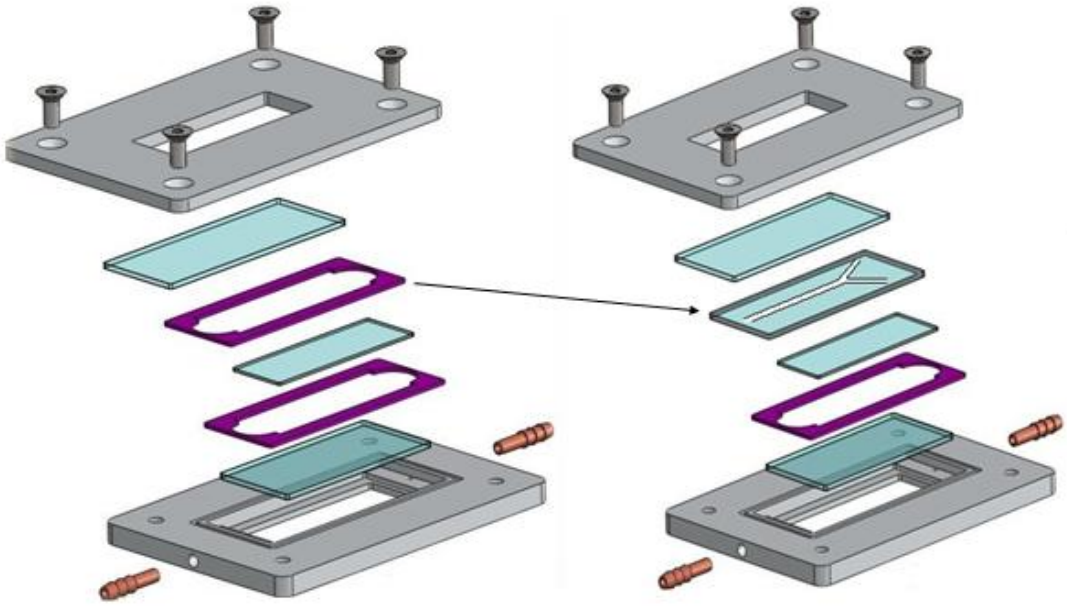

(b)

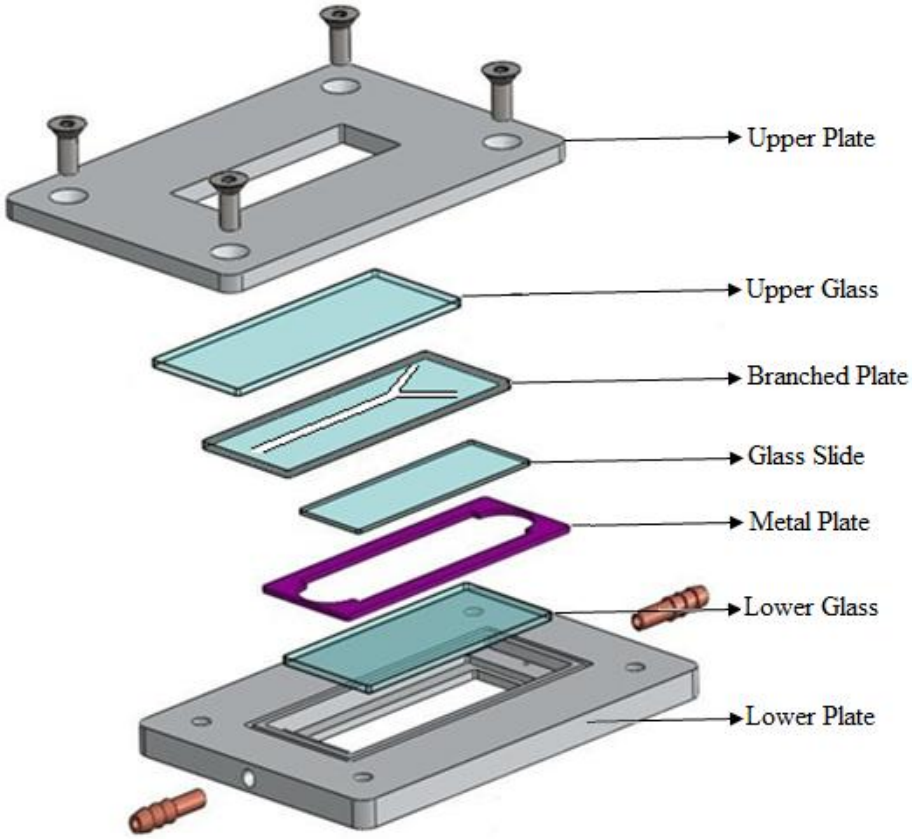

(c)

Figure 3.1 (Cont.)

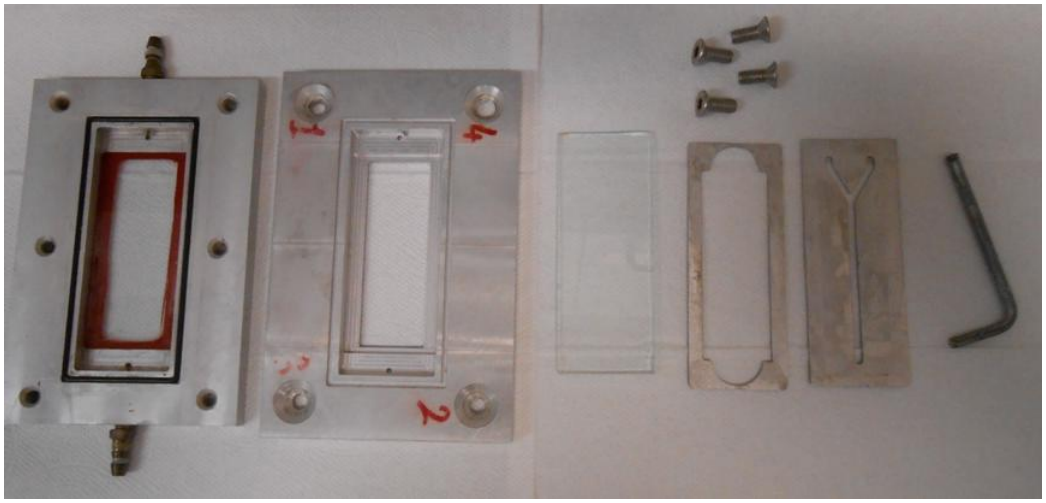

(d)

Figure 3.1 (Cont.)

The assembly of flow chamber was made in such a way that cells grown on glass slide was placed on the lower plate of chamber which was held firmly by the metal plate. On its top, branched plate was placed to mimic the shape of an artery and provide disturbed flow. The upper glass was then placed above branched plate and chamber was tightened by putting the final upper plate and screwed.

3.2 METHODS

The first requirement before initiating the experiment was to verify the flow to be disturbed in the new design of parallel plate flow chamber which contained branched region in the form of a channel. For our experiments, we needed the existence of disturbed flow over HUVECs to determine its effect on cells.

3.2.1 Verifying the Pattern of Disturbed Flow

In order to authenticate the presence of disturbed flow in branched kit, an experiment was designed in which 5μm PSP (Polyamide Seeding Particles) were used to follow the pattern of flow. In this experiment PSP were dissolved in distilled water to make a solution. The parallel plate flow chamber was connected to a reservoir bottle filled with distilled water, through peristaltic pump to initiate the flow. The chamber

was without any cells just with glass slide inside, continuously being observed under inverted microscope. While the peristaltic pump was set to a flow rate of 300 ml/min, the PSP were injected into the tubing connected to parallel plate flow chamber to track the pattern of flow. Then the flow rate was increased to 380 ml/min, and the flow pattern was recorded under microscope with the help of camera.

3.2.2 HUVECs

HUVECs are Human Umbilical Vein Endothelial Cells isolated from the endothelium of veins from umbilical cord. They were selected as our culture cells in order to study the function and pathology of endothelial cells regarding atherosclerosis. HUVECs were provided by courtesy of biology lab of Fatih University. They were taken in a cryovial from nitrogen tank.

3.2.3 Cell Culture

In order to initiate experiment, HUVECs were thawed by placing the cryovial in water bath at 37 ^{o}C for less than a minute. The cryoprotectant DMSO (Dimethyl Sulfoxide) is toxic for the cells at this temperature so precaution was taken not to leave the cells for more than a minute in water bath. These cells were then transferred to a 15ml centrifuge tube and 10 ml of DMEM/L-glutamine medium (containing 10% FBS and 1% penicillin/streptomycin) was added dropwise primarily to adapt the cells with this environment. The cells were then separated from medium by centrifugation at 2000g for 5 minutes. The supernatant was discarded and the pellet of cells was dissolved by pipetting in 1 ml of DMEM/L-glutamine medium (containing 10% FBS and 1% penicillin/streptomycin). This 1 ml of cell solution was spread on cell culture petri plate and 9 ml of fresh medium was added to it for their growth. The medium provides all the necessary growth factors and nutrients for the growth and multiplication of cells. The HUVECs were then placed in an incubator set at 37 ^{o}C and 5% CO_2 for 2-3 days unless they reached a confluency of 80-90%.

3.2.4 Subculturing of HUVECs

The HUVECs needed to be subcultured after 3 days when they reached a confluency of 80-90% due to increase of toxic metabolites, use of nutrients and increase in number of cells. In order to subculture the cells, the old medium was removed from

the petri plate. The HUVECs were washed with PBS (Phosphate Buffered Saline) in order to remove residual medium from the cells which may contain serum, Ca and Mg that inhibit the function of trypsin. 2 ml of trypsin, quite enough to cover whole surface was added into plate in order to cleave proteins that were binding HUVECs with the cultured dish. The petri plate was then placed in an incubator set at 37 ^{o}C for 4 minutes for the optimal activity of enzyme. Once the HUVECs were detached from cultured dish, 4 ml of fresh medium was added to it that was twice the amount of trypsin. The medium was added to inactivate trypsin by the serum present in it. The solution was mixed gently and then 1 ml of this was spread in a new petri plate. 9 ml of fresh medium was added to it and mixed well. The cells were placed in an incubator with the same conditions for another 2 days. After 2 passages, the HUVECs were ready for experiment.

3.2.5 Seeding of HUVECs on Glass Slide

Glass slide is suitable for cell culturing but it requires a coating to promote cell attachment. Cells need an extracellular matrix to adhere to glass slide. A variety of coating materials are available depending on cell types such as gelatin, fibronectin, poly-L-lysine, poly-D-lysine, collagen IV etc. For our cell types (HUVECs), gelatin was good enough for adherence. In order to find the optimal concentration of gelatin for HUVECs attachment on glass slide, a range of gelatin concentration was tested i-e. from 1 % to 7 %. The solution of gelatin was made in distilled water. The solutions were made according to the Table 3.3 and then autoclaved at 121 ^{o}C and 15 Psi for 20 minutes. It provided both the sterilization and helped the gelatin to be dissolved in distilled water.

Table 3.3 Concentration of gelatin ranging from 1 % to 7 %.

Concentration (%)	Gelatin Powder (g)	Distilled Water (ml)
1	0.5	50
2	1	50
3	1.5	50
4	2	50

Table 3.3 (Cont.)

5	2.5	50
6	3	50
7	3.5	50

After the formation of range of solutions, autoclaved glass slides were coated with these solutions in such a way that they covered the whole surface. The glass slides were then placed in an incubator for overnight to dry completely. Once the slides were absolutely dried, HUVECs were cultured on them in a similar way as was performed subculturing of cells. After 2-3 days when HUVECs reached the confluency of 80-90 % the cells were tested for their adherence and confluency. 2 % gelatin was found to be good enough for HUVECs adherence on glass slide.

3.2.6 Experimental Setup

Before performing experiment all the apparatus was autoclaved to sterilize them that included parallel plate flow chamber, reagent bottles and forceps. In order to carry out the flow experiment over HUVECs, the glass slide with attached cells was placed in the flow chamber with the help of sterile forceps. The flow chamber was assembled within the biosafety cabinet and connected with tubing to the two reagent bottles half filled with DMEM (Dulbecco's Modified Eagle Medium). One of the reagent bottles served as a damper and the other as reservoir. The use of two reagent bottles was to prevent the formation of bubbles in the experimental system which may interfere with the shear stress and affect the flow. After the assembly of whole setup in biosafety cabinet, the whole apparatus along with the reagent bottles was carefully taken out of cabinet and connected with peristaltic pump. The pump was set to a flow rate of 380 ml/min, calculated regarding desired shear stress of 12.28 dynes/cm^2 as the normal shear stress in arteries ranges from 10-70 dynes/cm^2. The flow chamber was placed under microscope to continuously observe the HUVECs for the change in their morphology, adherence and confluency. The photographs were taken with the gradual increase in time up to 24 hours and then they were compared for the identification of alterations occurred. The whole experimental setup is shown in Figure 3.2.

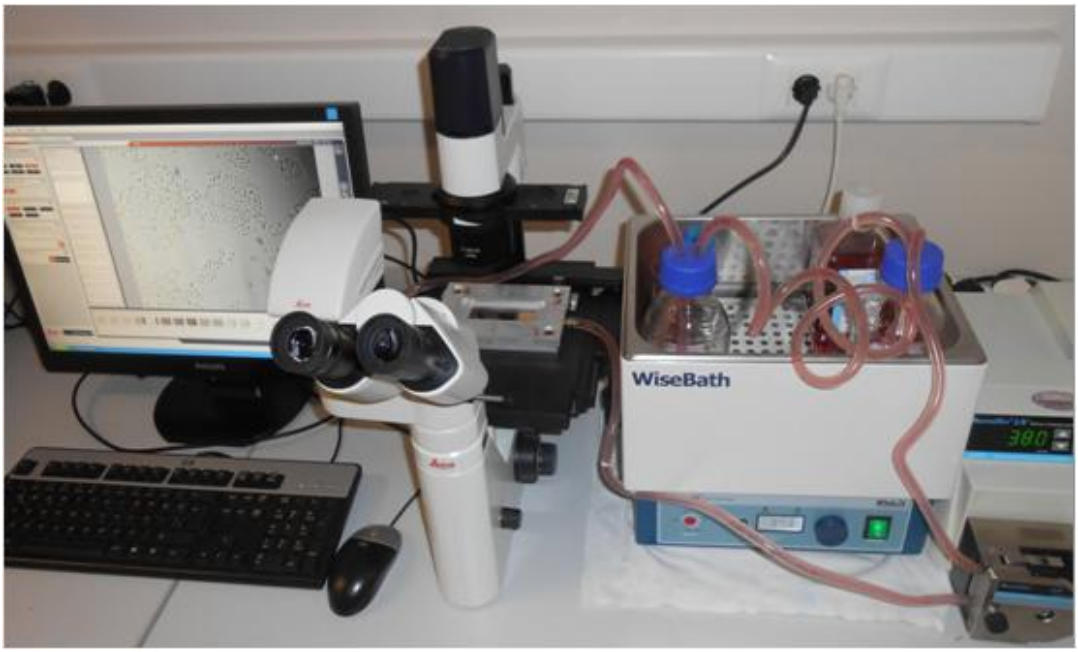

Figure 3.2 Experimental setup showing the HUVECs under flow in branched kit of parallel plate flow chamber connected to peristaltic pump under microscope.

The direction of flow through the branched plate was made to be coming from the straight region of channel and then bifurcating through the branched region as shown in Figure 3.3.

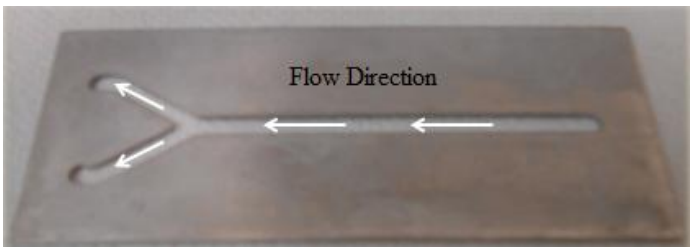

Figure 3.3 Direction of flow through branched plate over HUVECs under flow.

3.2.7 Problem

When the experiment was carried out, there was a problem of cell detachment. The HUVECs were continuously being detached from the glass slide under flow rate of 380 ml/min as is visible in Figure 3.4.

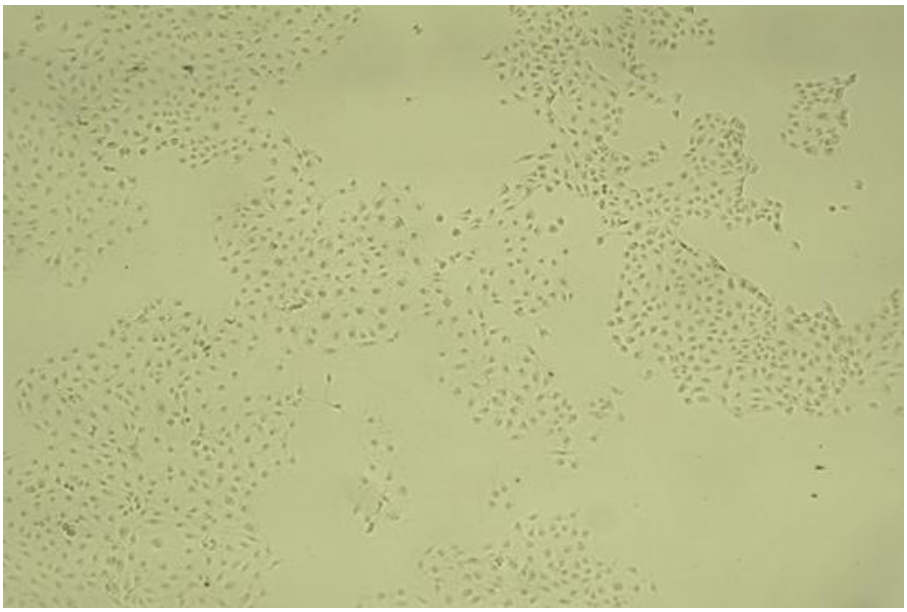

Figure 3.4 HUVECs detachment from glass slide under flow rate of 380 ml/min.

A scientific approach was made to resolve this issue. There were three apparent possibilities as a cause of this problem.

1. Glass slides were not good enough for cell adherence.
2. Flow rate was not dynamically simulated.
3. There could be a problem in branched plate dimensions.

So, all of these possibilities were tested by adapting following considerations.

3.2.7.1 Replacing Glass Slides

Thinking that there might be a problem in seeding of HUVECs on glass slide, it was decided to seed HUVECs on plastic slide. The petri plates are made up of plastic, having an additional coating for better adherence of cells on it. So, the slides were cut from petri plates to be used in place of glass slides. However, the plastic slides cannot be autoclaved for sterilization so they were sterilized with 70% ethanol. In order to test whether washing of plastic slides with ethanol has any affect on growth of HUVECs, HUVECs were grown on two petri plates one washed with ethanol and the other

without any washing. The results were quite good showing that there was no evident difference in growth of HUVECs over both plates as shown in Figure 3.5.

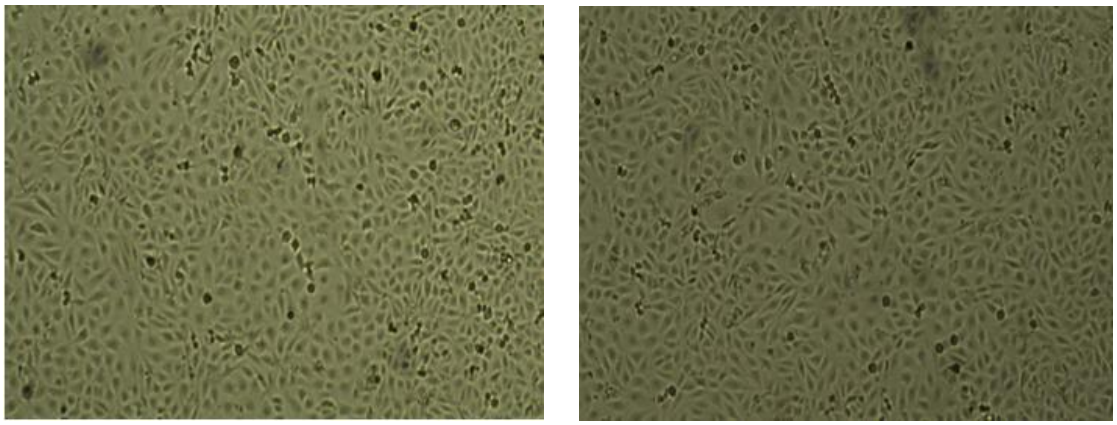

(a) (b)

Figure 3.5 Confluency of HUVECs grown on petri plate (a) without washing with ethanol (b) washed with ethanol.

HUVECs were then seeded on these self made plastic slides and they showed splendid confluency for carrying out the flow experiment. The confluency of HUVECs on plastic slides is shown in Figure 3.6.

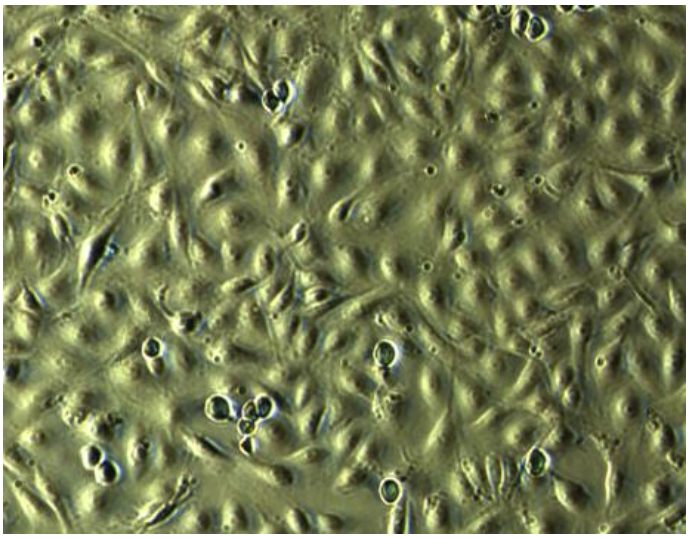

Figure 3.6 Confluency of HUVECs on plastic slide.

When the HUVECs were subjected to shear stress by applying flow over them, they again got detached from the plastic slide. The HUVECs were also seeded on coverslip and the glass slide treated with nitric acid (HNO_3) overnight in order to check the quality of adherence. The coverslip was used without any gelatinization but the HNO_3 treated glass slide was first gelatinized and then seeded with the cells. Both the coverslip and HNO_3 treated glass slide showed good confluency of HUVECs as shown in Figure 3.7 but the cells again failed to stand shear stress during flow experiment and got detached.

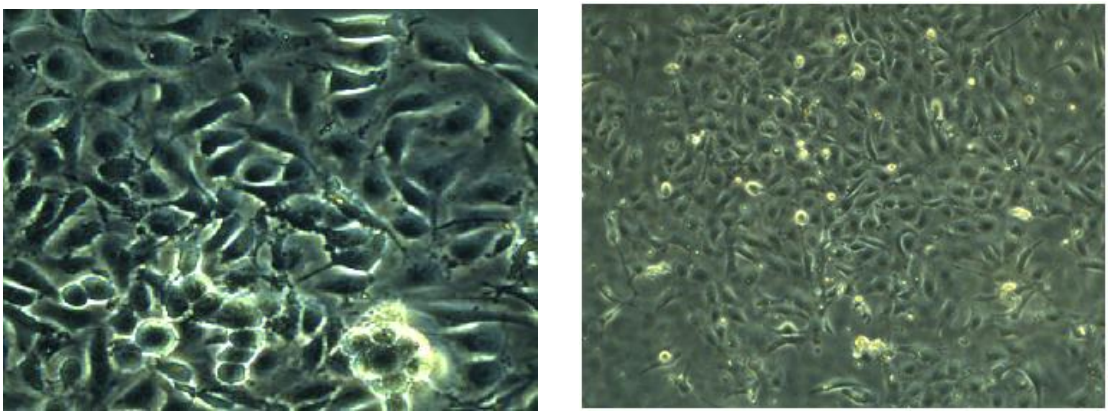

(a) (b)

Figure 3.7 Confluency of HUVECs on (a) Non-gelatinized coverslip, (b) Gelatinized glass slide treated with HNO_3.

3.2.7.2 Dynamic Simulation of Flow Rate

The flow rate was dynamically simulated in order to overcome the problem of cell detachment from the glass slide. The *in vitro* flow rate of DMEM over HUVECs was dynamically simulated with *in vivo* flow rate of blood in arteries. The Reynolds number for both the given *in vitro* DMEM and *in vivo* blood was compared and the flow rate was calculated that mimics the exact flow rate inside the body in coronary arteries.

Reynolds number is a dimensionless number which is a ratio of inertial forces to viscous forces [63]. It is defined according to Eq. (3.1).

$$Re = \frac{\rho UD}{\mu} \tag{3.1}$$

where Re is Reynolds number, ρ is density, U is velocity, D is diameter and μ is the dynamic viscosity.

Re can be modified as follows:

$$Re = \frac{\frac{\rho D4Q}{\pi D^2}}{\mu}$$

$$Re = \frac{4\rho Q}{\pi D\mu} \tag{3.2}$$

Applying dynamic simulation:

$$Re_{(in\ vivo\ \text{blood})} = Re_{(in\ vitro\ DMEM)}$$

Table 3.4 Parameters for blood and DMEM.

***in vivo* Blood**	***in vitro* DMEM**
$\rho = 1.06\ g/cm^3$	$\rho = 1\ g/cm^3$
$Q = 169\ ml/min$	Q =?
$D = 4.28\ mm$	$D = 3\ mm$
$\mu = 0.03\ dyne.sec/cm^2$	$\mu = 0.084\ dyne.sec/cm^2$

$$Q_{(in\ vitro\ DMEM)} = 35\,ml/min$$

The flow rate was calculated to be 35 ml/min according to dynamic simulation and the range of 35-50 ml/min of flow rate was used for experimentation. Despite of this simulation, HUVECs continue to detach from the surface of glass slide under flow.

3.2.7.3 Changing Dimensions of Branched Plate

After the trial of above mentioned remedies, when no success was seen to avoid cell detachment then an experiment was performed without the branched plate inside parallel plate flow chamber. The flow was laminar over HUVECs seeded on gelatinized glass slide and there was no cell detachment seen for more than 24 hours under the flow rate of 380 ml/min. This suggested that the problem was not in the seeding of HUVECs on glass slide or the flow rate but with the dimensions of branched plate.

So, the dimensions of branched plate were kept into consideration. The volume provided by the branched channel was not enough for the survival and adherence of HUVECs on slides. The width of the channel was 3 mm only. HUVECs like all other cells depend on neighboring cells for their support and attachment. The cells living in one area hold one another through extracellular matrix and nourish together. When the HUVECs under the shaded area of branched plate died due to high pressure and no nutrients, then the extracellular support provided by them to the cells inside channel was also diminished. The HUVECs inside the channel then were unable to hold on any support and bear high flow rate that's why they continue to detach with the medium passing over them. So, it was pondered to increase the diameter of branched plate and the new plate was manufactured with the width of 10 mm. The dimensions of the new branched plate in comparison with the old one is shown in Figure 3.8.

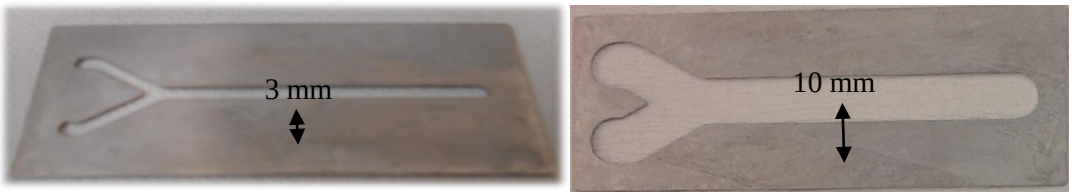

(a) (b)

Figure 3.8 Modification in dimensions of branched plate (a) Old plate with the width of 3 mm (b) New plate with the width of 10 mm.

To increase the height of the channel, two instead of one branched plate was used. The experiment was then carried out with the modified branched plate inside parallel plate flow chamber together with dynamic simulation for the new dimensions and there was no detachment of HUVECs observed under microscope. The HUVECs were subjected to shear stress of 12.28 dynes/cm^2 by adjusting the flow rate to 100 ml/min according to dynamic simulation. HUVECs remained under disturbed flow for 24 hours. Subsequently the cells from the glass slide were successfully collected separately from the region that were under laminar and disturbed flow, and stored at -80 ^{o}C until the isolation of RNA. For comparison studies, HUVECs were also subjected to laminar flow for 24 hours and under static conditions without any flow for 24 hours. So, we had four groups of HUVECs for PCR analysis that were HUVECs under:

1. Static conditions.
2. Laminar flow for 24 hours in parallel plate flow chamber without branch plate inside.
3. Disturbed flow region for 24 hours in branched parallel plate flow chamber.
4. Laminar flow region for 24 hours in branched parallel plate flow chamber.

All of these cells were collected carefully and stored at -80 ^{o}C for further analysis that include the isolation of RNA from HUVECs, synthesis of cDNA from RNA and finally carrying out PCR reactions for identifying genes that were expressed or down regulated under different flow conditions.

3.2.8 Total RNA Isolation

TRIpure reagent was used for the isolation of total RNA from HUVECs exposed to static conditions, laminar flow and disturbed flow. Total RNA, DNA and proteins from the same sample can be isolated in a single step liquid phase separation by using TRIpure reagent [64]. The method is the modification of single step RNA isolation procedure which was developed by Chomczynski and Sacchi [65]. TRIpure reagent is a ready to use reagent containing mono phasic solution of phenol and guanidine isothiocyanate which maintains the integrity of RNA by denaturing endogenous

nucleases while disrupting the cells. For the isolation of total RNA from the HUVECs, the cells were first centrifuged to separate them for the storage media. After centrifugation the procedure adapted for RNA isolation was a modification of Roche's nucleic acid isolation and purification manual. The pellet of HUVECs for every group (static, laminar, disturbed flow) was dissolved in 500 µl of TRIpure solution and incubated at room temperature for 5 minutes to dissociate nucleoprotein complexes. After that, 100 µl of chloroform was added into the tube which was vortexed and incubated at room temperature for 10 minutes. The incubation was followed by centrifugation at 12,000 x *g* for 15 minutes at 4 ^{o}C as a result of which three different phases were formed namely the top colorless phase containing RNA, white interphase containing DNA and the bottom red phase containing proteins. The top colorless phase containing RNA was transferred into new eppendorf tube and centrifuged at 12,000 x *g* for 15 minutes at 4 ^{o}C to remove any phenol residual. For the precipitation of total RNA content, the supernatant containing RNA was transferred to another eppendorf tube and 250 µl of isopropanol was added to it. It was mixed gently and incubated at room temperature for 10 minutes followed by centrifugation at 12,000 x *g* for 10 minutes at 4 ^{o}C. Supernatant was discarded and the pellet was then washed with 500 µl of 75 % ethyl alcohol and centrifuged at 7500 x *g* for 5 minutes at 8 ^{o}C. Supernatant was discarded and 1 ml of RNase free water was added to the tube. The total RNA content for each sample was then found by nanodrop spectrophotometer and recorded as shown in Table 3.5. The total RNA samples of HUVECs were stored at -80 ^{o}C until cDNA synthesis.

Table 3.5 RNA content in different samples.

Samples	**Concentration (ng/µl)**
Static	205
Laminar Flow (24 hours)	13.6
Branched Region	38
Linear Region	19

3.2.9 cDNA Synthesis

For the synthesis of cDNA, miScript II RT Kit was used. The kit consists of 5x miScript HiSpec buffer, 10x nucleic mix, RNase free water and miScript reverse transcriptase mix. Total RNA containing miRNA was used as a starting material for cDNA synthesis. The recommended RNA input to synthesize cDNA for future miRNA profiling is 250-500 ng. The template RNA was thawed on ice while 10x nucleic mix and 5x miScript HiSpec buffer were thawed at room temperature. The reverse transcription master mix was prepared on ice depending upon the concentration of different samples in Table 3.6.

Table 3.6 Reverse transcription master mix for cDNA synthesis.

Components	**Static**	**Laminar Flow (24 hours)**	**Branched Region**	**Linear Region**
5x miScript HiSpec Buffer	4 µl	4 µl	4 µl	4 µl
10x Nucleics Mix	2 µl	2 µl	2 µl	2 µl
RNase-free water	9 µl	0 µl	5 µl	0 µl
miScript Reverse Transcriptase Mix	2 µl	2 µl	2 µl	2 µl
Template RNA	3 µl (615 ng)	12 µl (163.2 ng)	7 µl (266 ng)	12 µl (228 ng)
Total Volume	20 µl	20 µl	20 µl	20 µl

The entire preparation of master mix was made on ice. miScript reverse transcriptase mix was removed from -20 ^{o}C just before the preparation of master mix and immediately returned to the freezer after use. The template RNA for each sample was added at the end of reaction mixture in each tube. The tubes were mixed gently and briefly centrifuged, then placed on ice. After that the samples were incubated at 37 ^{o}C for 60 minutes. For the inactivation of miScript reverse transcriptase mix, the samples were incubated at 95 ^{o}C for 5 minutes and placed on ice.

3.2.10 miRNome Analysis through qPCR

The Human miRNome miScript miRNA PCR Array was utilized for expression analysis that consisted of 12 different PCR array plates each having 96 wells. Only first plate was used for studying the expression of 96 different genes. The miScript miRNA PCR Array plate layout is shown in Figure 3.9. In the plate, wells A1 to G12 contained miScript primer assay for pathway related miRNA. Wells H1 and H2 contained replicate *C. elegans* miR-39 miScript primer assays that served as an alternative normalizer for array data. Wells H3 to H8 contained assay for housekeeping genes that served as a normalization control. Wells H9 and H10 contained replicate reverse transcription controls (miRTC). Wells H11 and H12 contained replicate positive PCR controls (PPC).

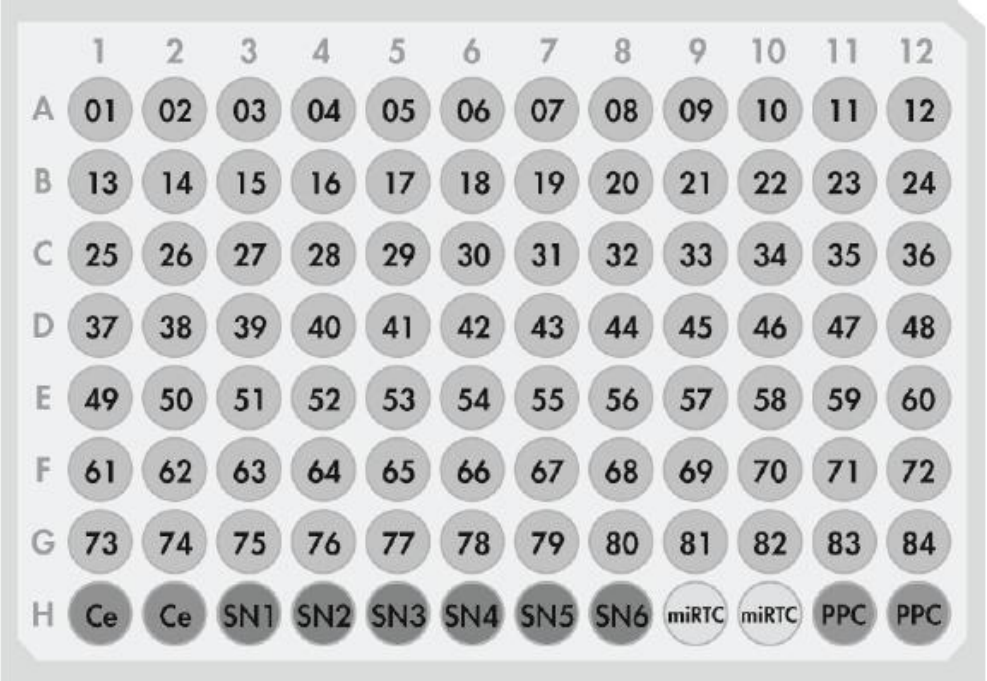

Figure 3.9 miScript miRNA PCR array plate layout [66].

The purpose of different controls in miScript PCR Array is as follows [66]:

1.1 *C. elegans* miR-39 miScript Primer Assay was used as alternative data normalization by utilizing exogenously spiked Syn-cel-miR-39 miScript miRNA Mimic.

2.1 6 snoRNA/snRNA miScript Primer Assays (miScript PCR Controls) were used for data normalization by using $\Delta\Delta C_T$ of relative quantification.

3.1 miRTC were used for the assessment of reverse transcription.

4.1 PPC were used for the assessment of PCR performance.

The cDNA synthesized by reverse transcription reaction using miScript HiSpec Buffer served as a template for quantitative PCR analysis. Before the start of human miRNA expression analysis through qPCR also called real time PCR, 20 µl of synthesized cDNA was diluted in 500 µl of RNase free water. Real time PCR profiling of mature miRNA was done using miScript miRNA PCR array together with miScript SYBR Green PCR kit that contained miScript universal primer (reverse primer) and QuantiTect SYBR Green PCR master mix. In order to prepare the reaction mix for real time PCR, miScript miRNA PCR array was carefully removed from its sealed bag. The dilution was made with 15 µl of RNase free water which was then distributed for three sets each having 5 µl of primer in PCR tubes. QuantiTect SYBR Green PCR master mix, miScript universal primer, template cDNA and RNase free water were thawed at room temperature. The reaction mix was then prepared for each PCR tube according to the Table 3.7.

Table 3.7 Reaction mix for miRNome miScript miRNA PCR Array.

Sr. No.	**Component**	**Quantity (µl)**
1	QuantiTect SYBR Green PCR Master Mix	7.5
2	miScript Universal Primer	1
3	RNase free water	0.5
4	Template cDNA	1
5	Forward Primer	5
Total Volume		15 µl

After the preparation of reaction mix, it was carefully transferred into PCR tubes with proper labeling from A1 to H12. PCR tubes were then placed in real time cycler, programmed according to Table 3.8. The same procedure was carried out for qPCR of four samples of interest.

Table 3.8 Cycling conditions for real time PCR.

Step	Time	Temperature	Comments
PCR initial activation step	15 min	95^{o}	For the activation of Taq DNA polymerase
Denaturation	10 sec	95^{o}	Causes DNA melting to form single stranded DNA
Annealing	15 sec	60^{o}	Annealing of primers to single stranded DNA
Extension	15 sec	72^{o}	For fluorescence data collection
Cycle number	42 cycles		It depends on the concentration of template cDNA

3.2.11 Data Analysis using ΔΔCt Method

Real time PCR instrument gave us the Ct values for all respective genes in four different samples which were exported for ΔΔCt analysis. Ct (cycles of threshold) is a relative value that corresponds to cycle number at which amount of amplified DNA reaches threshold level [67]. The same threshold was defined for each sample in order to have relative comparison. The amplification of housekeeping genes was observed which was utilized for normalization by calculating ΔCt values for each sample.

$$\Delta Ct = Ct\ (housekeeping) - Ct\ (sample)$$

High ΔCt represents low expression while low ΔCt represents highly expressed genes [64]. For comparison of differences in gene expression between HUVECs exposed to disturbed flow and laminar flow, ΔΔCt values were calculated by subtracting ΔCt (disturbed) from ΔCt (laminar).

$$\Delta\Delta Ct = \Delta Ct\,(\text{laminar}) - \Delta Ct\,(\text{disturbed})$$

The absolute values of ΔΔCt were then taken for calculating fold change. Fold change represents the expression ratio.

$$\text{Fold change} = 2^{-\Delta\Delta Ct}$$

After ΔΔCt analysis, values higher than +5 were regarded as downregulated and lesser than -5 were referred to as upregulated. The affected genes were then searched in databases (miRNA Database) for their probable function in relation to endothelial cell function and their role in causing atherosclerosis.

CHAPTER 4

RESULTS

4.1 VERIFYING THE PATTERN OF DISTURBED FLOW

During the experimentation, images were captured repeatedly with the help of Leica application suite and digital camera The flow experiment with distilled water containing dissolved 5µm PSP at a flow rate of 300 ml/min and 380 ml/min showed a clear pattern of flow under inverted microscope At a flow rate of 300 ml/min, the particles were first showing laminar flow and as soon as they reached the branch point they showed a clear divergence around curvature as shown in Figure 4.1 (a)

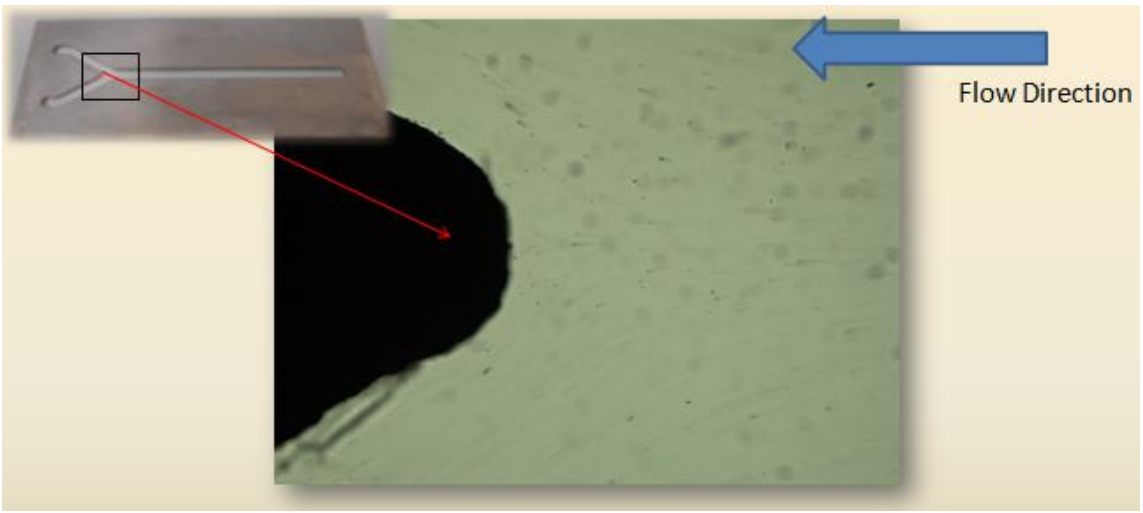

(a)

Figure 4.1 Verification of pattern of disturbed flow in branched kit of parallel plate flow chamber. (a) At flow rate 300 ml/min, the 5µm PSP were diverging at branched point. (b) At high flow rate of 380 ml/min, 5µm PSP showed a clear disturbed flow pattern at branched point.

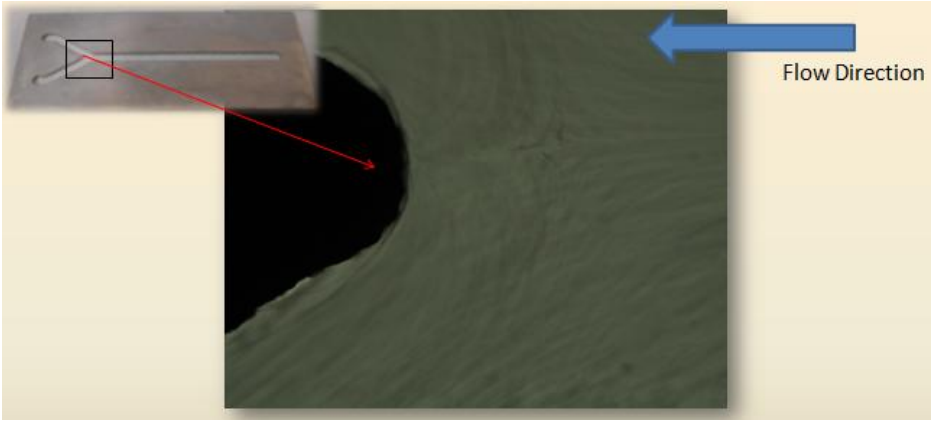

(b)

Figure 4.1 (Cont.)

At a higher flow rate of 380 ml/min, the flow was laminar in the beginning and near branching region there was first flow separation then recirculation followed by reattachment region which is magnificently pictured in Figure 4.1 (b).

4.2 ACCUMULATION OF MATERIALS AROUND BRANCH POINT

During this experiment, it was also observed that there was accumulation of some materials around branching point along with the flow at a rate of 280 ml/ min. This accumulation suggests the possibility of deposition of fatty materials at this region which provides them more time span for inducing signal transduction here, indirectly causing atherosclerosis. The deposition of materials is shown in Figure 4.2.

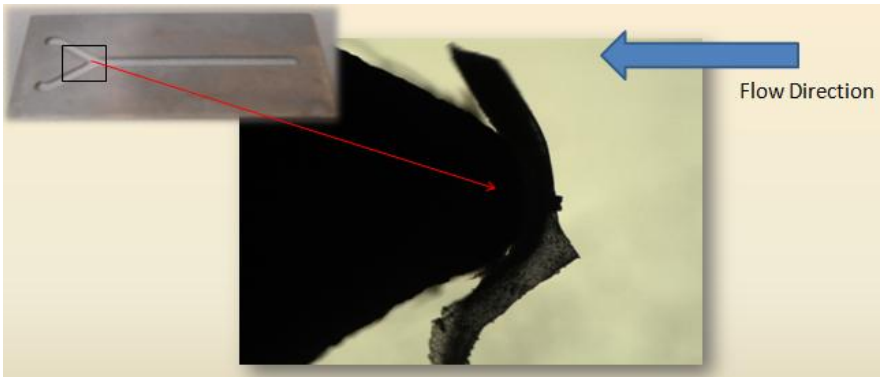

Figure 4.2 Accumulation of materials around branch point suggesting the chance of deposition of fatty materials at this region. Flow rate 280 ml/min.

4.3 CONFLUENCY OF HUVECS

For experimentation, the HUVECs needed to be confluent enough (80-90 %) for subculturing and their seeding on glass slide. The confluency of HUVECs in petri plates observed under microscope is shown in Figure 4.3.

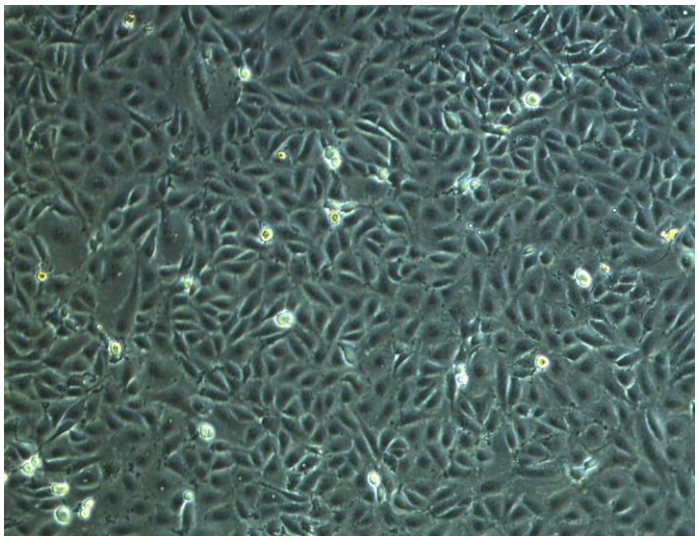

Figure 4.3 Confluency of HUVECs on petri plate observed under microscope (10X).

4.4 TRYPSINIZATION OF HUVECS

Subculturing of adherent cells required the cells to be detached from the growing surface which was done by treating the cells with enzyme like trypsin. It cleaved the bond between cells and adherent surface without affecting the cells. Once the HUVECs were detached from petri plate after trypsinization, they were easily subcultured and seeded on glass slide. The Figure 4.4 shows the HUVECs after treating with trypsin for their detachment.

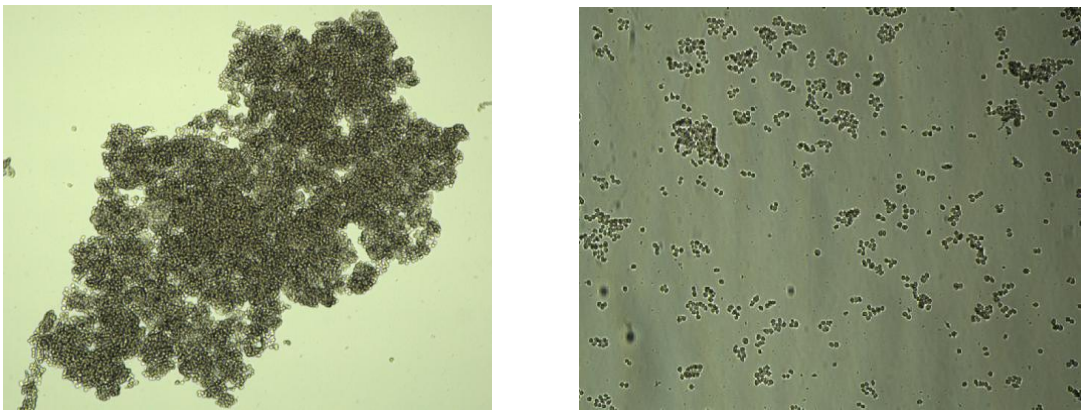

(a) (b)

Figure 4.4 Trypsinization of HUVECS (a) Clump of detached HUVECs after treating with trypsin, (b) After agitation, separation of HUVECS.

4.5 SEEDING OF HUVECS ON GLASS SLIDE

HUVECs were grown on glass slide so that they can be put in parallel plate flow chamber. The glass slides were first gelatinized with 2 % gelatin and HUVECS then grown on them. The Figure 4.5 shows the confluency of HUVECs on gelatinized glass slide. This slide was then placed in parallel plate flow chamber with the branched plate inside it, mimicking the coronary artery, and flow was applied over HUVECs.

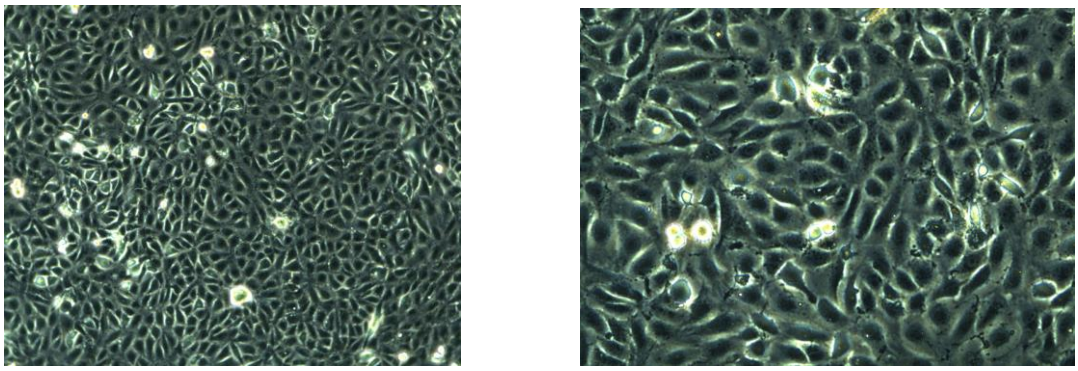

(a) (b)

Figure 4.5 Confluency of HUVECs on gelatinized glass slide (a) 10X resolution, (b) 20X resolution.

4.6 MORPHOLOGICAL CHANGES IN HUVECS UNDER FLOW

As reported by many researchers, endothelial cells tend to elongate in the direction of flow, we observed the similar results for laminar flow experiment. On the other hand for disturbed flow experiment, the morphological changes observed were quite unusual. The cells in the region of flow separation and reattachment were under continuous disturbed flow as a result of which the morphology of HUVECs was haphazard. For the disturbed flow experiment four different regions were analyzed for morphological changes. These four regions are shown in Figure 4.6. Region 1 is the area of flow separation where the flow is disturbed and bifurcating into two branches. Regions 2 and 3 are the regions of flow reattachment in upper and lower branched artery respectively. Region 4 is the area of plate with laminar flow and no flow disturbance.

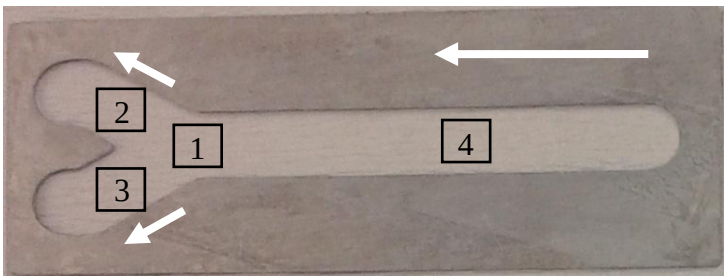

Figure 4.6 Different regions of branched plate depending on flow pattern. Region 1 is flow separation area, regions 2 and 3 are flow reattachment areas and region 4 is laminar flow area.

The morphology of HUVECs under different regions during various time intervals were captured and then compared which can be seen in Figure 4.7. The arrow indicates the direction of flow.

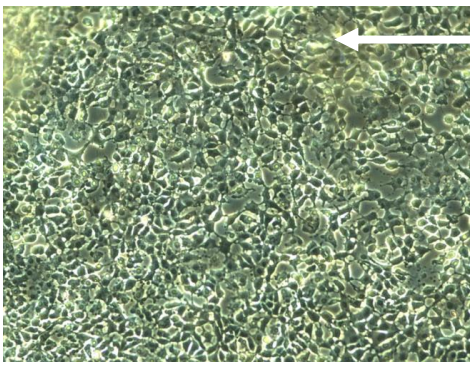

t = 0 minute

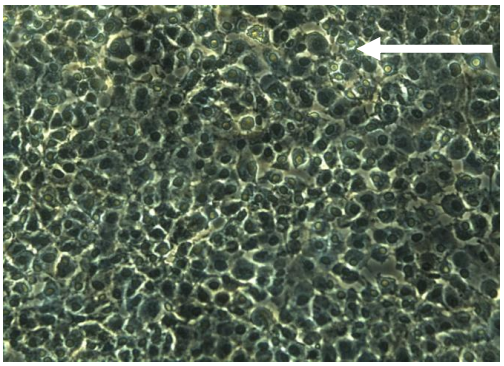

t = 1 hour

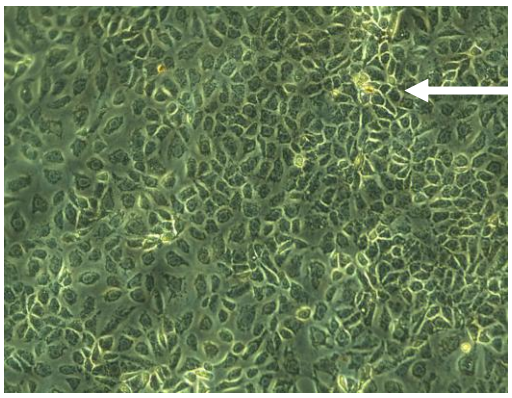

t = 24 hours

(a)

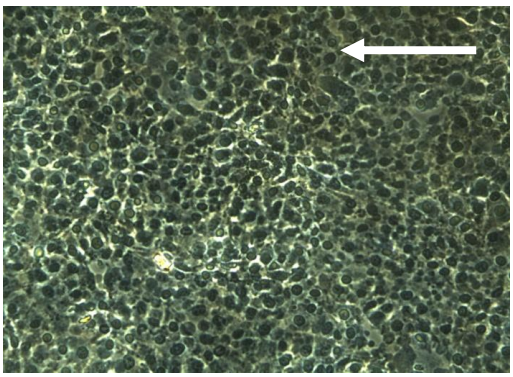

t = 0 minute

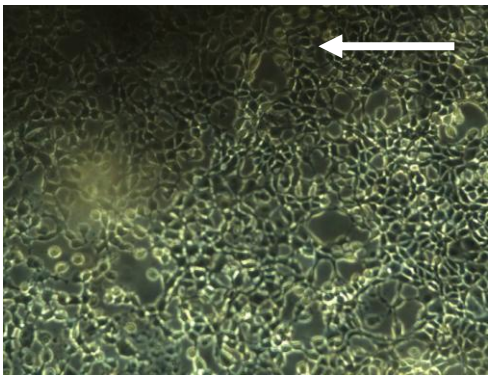

t = 1 hour

Figure 4.7 Morphological changes in HUVECs under flow rate of 100 ml/min in different regions of branched parallel plate flow chamber. (a) Region 1, (b) Region 2, (c) Region 3 and (d) Region 4.

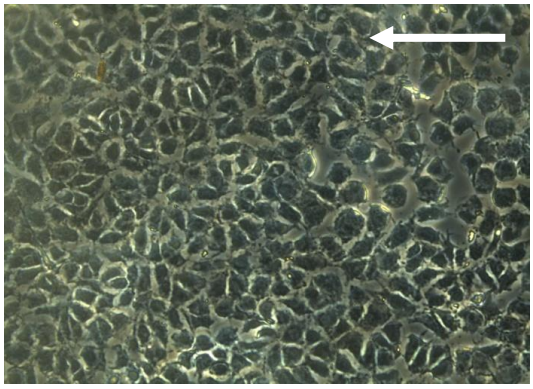

t = 24 hours

(b)

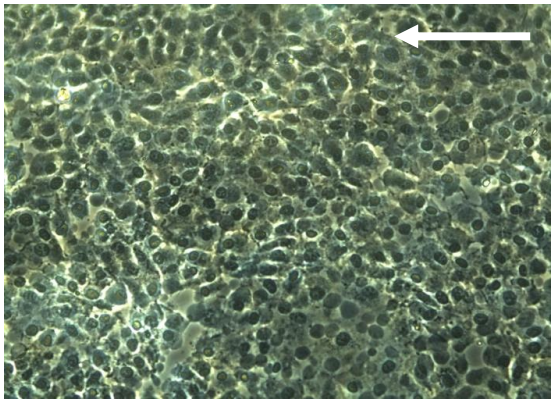

t = 0 minute

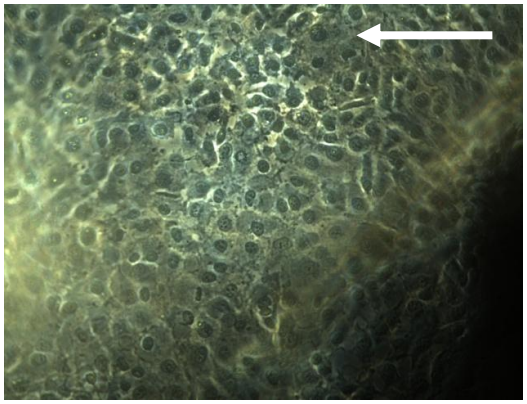

t = 1 hour

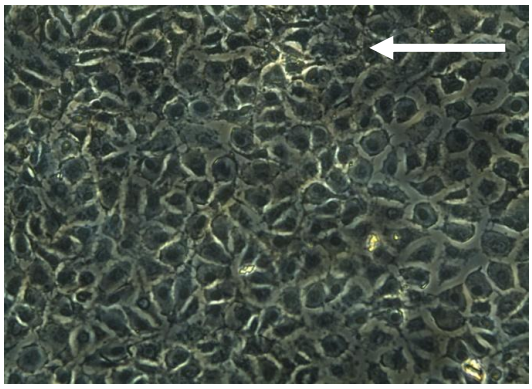

t = 24 hours

(c)

Figure 4.7 (Cont.)

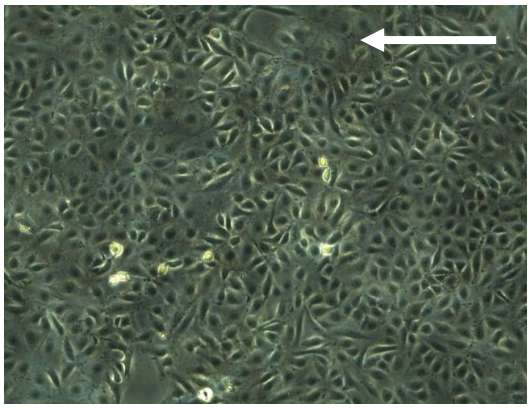

t = 0 minute

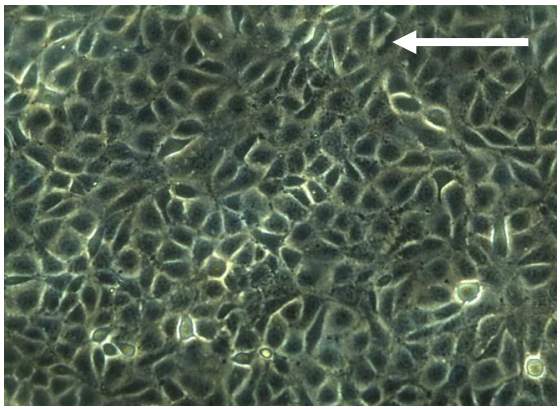

t = 1 hour

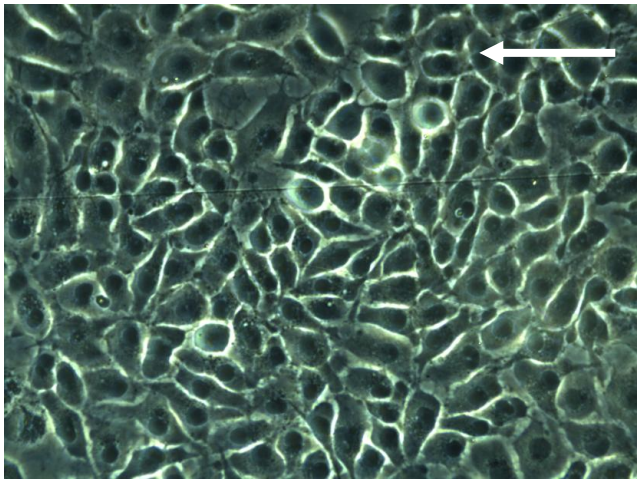

t = 24 hours

(d)

Figure 4.7 (Cont.)

After 24 hours of flow experiment on HUVECs, the morphological change in cells exposed to disturbed flow in region 1 was more evident in the form of round shape. Regions 2 and 3 which were flow reattachment regions showed dissociation of cells because of eddy currents in these regions. The morpholgy of HUVECs in these regions were tending to be spherical. Region 4 were under laminar flow and the morphology of HUVECs in this region were elongated in the direction of flow as expected.

4.7 miRNome ANALYSIS THROUGH qPCR

Quantitation data of PCR cycler showed a plot between cycle number (x-axis) and fluorescence (y-axis) in order to display Ct values for each miRNA sequence, showing amplification (Figure 4.8). Every specific gene was given a specific colour depending on fluorescence so they were distinguishable. Before analyzing the results, threshold line was defined in order to specify the point of amplification initiation. The threshold line was set same for all samples. The amplification curves which started after 15 cycles showed specific amplification as no amplification of genes is possible before 15 cycles. The curves showing amplification after 35 cycles were for non specific amplification showing very low concentration of genes.

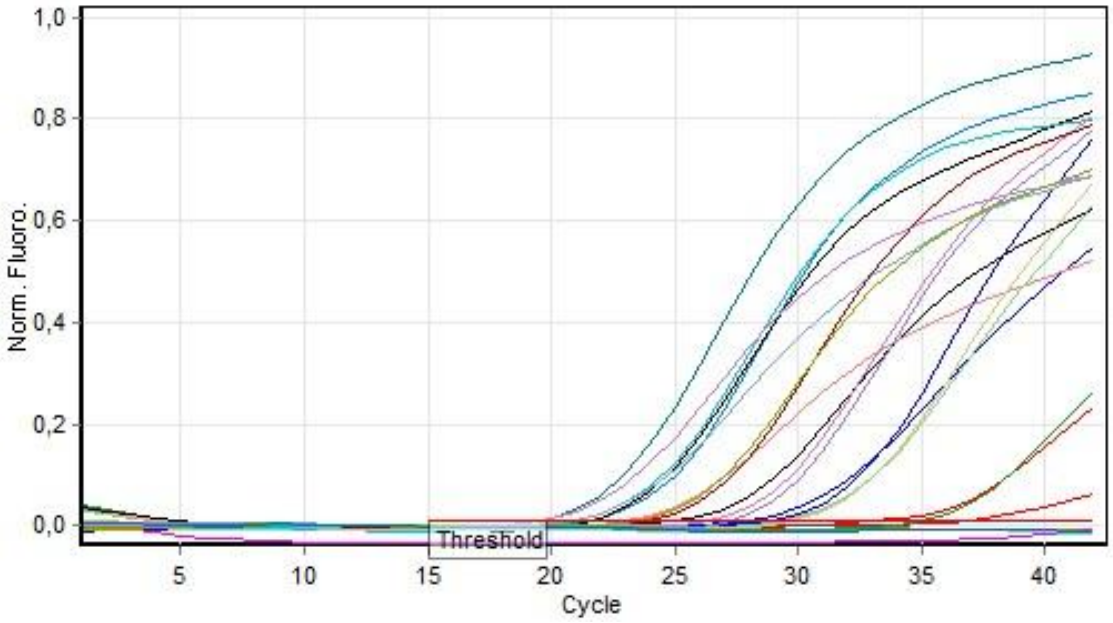

Figure 4.8 Plot between cycle number and fluorescence emission during PCR amplification.

Ct values define the point of intersection of amplification curve with the threshold line, hence defining the amplification level of genes. In miRNome analysis through qPCR, sets of Ct values were obtained for each sample. Low Ct value means high amplification and high Ct value means low amplification and sometimes non-specific amplification of genes (see Table 4.1)

Table 4.1 Quantitation data of PCR Cycler showing Ct values for specific well number.

No.	Colour	Well	Ct
1		A1	36.87
2		A2	33.38
3		A3	27.93
4		A4	28.91
5		A5	25.16
6		A6	21.5
7		A7	19.42
8		A8	23.04
9		A9	35.07
10		A10	42
11		A11	21.72
12		A12	21.09
13		B1	29.78
14		B2	29.37
15		B3	42
16		B4	20.8
17		B5	27.31
18		B6	19.42
19		B7	26.35
20		B8	23.76
21		B9	42
22		B10	23.33
23		B11	42
24		B12	42

The similar plots and Ct values were recorded for all the four samples namely: static, laminar 24 hrs (without branched plate), linear region and branched region (with branched plate). After applying ΔΔCt analysis and comparing disturbed flow region with laminar flow region, 22 different miRNAs were found to be affected in expression. 9 miRNAs were downregulated (shown in pink) and 13 miRNAs were upregulated (shown in green) according to Table 4.2.

Table 4.2 Data Analysis using ΔΔCt Method.

miRNA ID	Well	Static/ Control	Laminar 24hr Flow	Laminar Flow Region	Disturbed Flow Region	ΔCt Laminar Flow Region	ΔCt Disturbed Flow Region	ΔΔCt	ABS	Fold Change = 2^-ΔΔCt
		Ct(c)	Ct(f)	Ct(f)	Ct(f)					
hsa-miR-142-5p	A01	36.87	42	30.9	42	-1.1	-9.71	8.61	8.61	390.72
hsa-miR-9	A02	33.38	42	42	42	-12.2	-9.71	-2.49	2.49	5.62
hsa-miR-150	A03	27.93	42	33.48	42	-3.68	-9.71	6.03	6.03	65.34
hsa-miR-27b	A04	28.91	42	42	42	-12.2	-9.71	-2.49	2.49	5.62
hsa-miR-101	A05	25.16	42	40.85	42	-11.05	-9.71	-1.34	1.34	2.53
hsa-let-7d	A06	21.5	42	42	42	-12.2	-9.71	-2.49	2.49	5.62
hsa-miR-103a	A07	19.42	42	41.14	42	-11.34	-9.71	-1.63	1.63	3.10
hsa-miR-16	A08	23.04	42	34.38	39.71	-4.58	-7.42	2.84	2.84	7.16
hsa-miR-26a	A09	35.07	42	42	42	-12.2	-9.71	-2.49	2.49	5.62
hsa-miR-32	A10	42	42	42	42	-12.2	-9.71	-2.49	2.49	5.62
hsa-miR-26b	A11	21.72	42	42	42	-12.2	-9.71	-2.49	2.49	5.62
hsa-let-7g	A12	21.09	42	32.14	36.28	-2.34	-3.99	1.65	1.65	3.14
hsa-miR-30c	B01	26.01	42	42	36.23	-12.2	-3.94	-8.26	8.26	306.55
hsa-miR-96	B02	29.37	42	17.99	42	11.81	-9.71	21.52	21.52	3007222.1
hsa-miR-185	B03	42	42	24.11	42	5.69	-9.71	15.4	15.4	43237.64
hsa-miR-142-3p	B04	20.8	42	29.74	42	0.06	-9.71	9.77	9.77	873.10
hsa-miR-24	B05	27.31	42	33.99	37.38	-4.19	-5.09	0.9	0.9	1.87
hsa-miR-155	B06	19.42	42	30.44	42	-0.64	-9.71	9.07	9.07	537.45
hsa-miR-146a	B07	26.35	42	32.46	36.83	-2.66	-4.54	1.88	1.88	3.68
hsa-miR-425	B08	23.76	42	34.14	42	-4.34	-9.71	5.37	5.37	41.36
hsa-miR-181b	B09	42	42	41.1	35.24	-11.3	-2.95	-8.35	8.35	326.29
hsa-miR-302b	B10	23.33	42	42	42	-12.2	-9.71	-2.49	2.49	5.62
hsa-miR-30b	B11	42	42	34.05	42	-4.25	-9.71	5.46	5.46	44.02
hsa-miR-21	B12	42	34.75	30.63	32.51	-0.83	-0.22	-0.61	0.61	1.53
hsa-miR-30e	C01	25.03	42	38.29	42	-8.49	-9.71	1.22	1.22	2.33
hsa-miR-200c	C02	24.8	42	38.76	42	-8.96	-9.71	0.75	0.75	1.68
hsa-miR-15b	C03	20.17	42	34.14	33.66	-4.34	-1.37	-2.97	2.97	7.84
hsa-miR-223	C04	42	42	42	42	-12.2	-9.71	-2.49	2.49	5.62
hsa-miR-194	C05	29.19	42	42	42	-12.2	-9.71	-2.49	2.49	5.62
hsa-miR-210	C06	29.31	42	42	42	-12.2	-9.71	-2.49	2.49	5.62
hsa-miR-15a	C07	27.08	42	42	42	-12.2	-9.71	-2.49	2.49	5.62
hsa-miR-181a	C08	27.71	42	42	42	-12.2	-9.71	-2.49	2.49	5.62
hsa-miR-125b	C09	27.21	42	42	42	-12.2	-9.71	-2.49	2.49	5.62
hsa-miR-99a	C10	32.91	42	42	42	-12.2	-9.71	-2.49	2.49	5.62
hsa-miR-28-5p	C11	30.03	42	42	42	-12.2	-9.71	-2.49	2.49	5.62
hsa-miR-320a	C12	23.53	42	42	36.09	-12.2	-3.8	-8.4	8.4	337.79
hsa-miR-125a-5p	D01	20.23	42	35.77	32.98	-5.97	-0.69	-5.28	5.28	38.85
hsa-miR-29b	D02	26.36	42	42	42	-12.2	-9.71	-2.49	2.49	5.62
hsa-miR-29a	D03	20.69	42	42	35.09	-12.2	-2.8	-9.4	9.4	675.59
hsa-miR-141	D04	36.54	42	42	42	-12.2	-9.71	-2.49	2.49	5.62
hsa-miR-19a	D05	28.53	42	42	42	-12.2	-9.71	-2.49	2.49	5.62
hsa-miR-18a	D06	28.49	42	42	42	-12.2	-9.71	-2.49	2.49	5.62
hsa-miR-374a	D07	31.43	42	42	41.25	-12.2	-8.96	-3.24	3.24	9.45
hsa-miR-423-5p	D08	25.05	42	42	42	-12.2	-9.71	-2.49	2.49	5.62
hsa-let-7a	D09	39.16	42	42	42	-12.2	-9.71	-2.49	2.49	5.62
hsa-miR-124	D10	32.85	42	42	37.99	-12.2	-5.7	-6.5	6.5	90.51
hsa-miR-92a	D11	19.25	42	42	36.19	-12.2	-3.9	-8.3	8.3	315.17
hsa-miR-23a	D12	20.85	41.55	36.48	33.96	-6.68	-1.67	-5.01	5.01	32.22

Table 4.2 (Cont.)

miRNA ID	Well #	Static/ Control	Laminar 24hr Flow	Laminar Flow Region	Disturbed Flow Region	ΔCt Laminar Flow Region	ΔCt Disturbed Flow Region	ΔΔCt	ABS	Fold Change = 2^-ΔΔCt
hsa-miR-25	E01	21.79	42	37.02	34.54	-7.22	-2.25	-4.97	4.97	31.34
hsa-let-7e	E02	42	42	42	42	-12.2	-9.71	-2.49	2.49	5.62
hsa-miR-376c	E03	42	42	42	42	-12.2	-9.71	-2.49	2.49	5.62
hsa-miR-126	E04	29.78	42	17.36	37.95	12.44	-5.66	18.1	18.1	280958.98
hsa-miR-144	E05	42	42	42	42	-12.2	-9.71	-2.49	2.49	5.62
hsa-miR-424	E06	24.15	42	42	42	-12.2	-9.71	-2.49	2.49	5.62
hsa-miR-30a	E07	24.73	42	42	38.59	-12.2	-6.3	-5.9	5.9	59.71
hsa-miR-23b	E08	25.81	42	42	36.79	-12.2	-4.5	-7.7	7.7	207.94
hsa-miR-151-5p	E09	23.06	42	42	39.2	-12.2	-6.91	-5.29	5.29	39.12
hsa-miR-195	E10	23.28	42	33.33	36.33	-3.53	-4.04	0.51	0.51	1.42
hsa-miR-143	E11	42	42	42	42	-12.2	-9.71	-2.49	2.49	5.62
hsa-miR-30d	E12	24.77	41.27	42	42.13	-12.2	-9.84	-2.36	2.36	5.13
hsa-miR-191	F01	42	36.35	39.26	36.83	-9.46	-4.54	-4.92	4.92	30.27
hsa-let-7i	F02	25.96	42	42	42	-12.2	-9.71	-2.49	2.49	5.62
hsa-miR-302a	F03	42	42	42	42	-12.2	-9.71	-2.49	2.49	5.62
hsa-miR-222	F04	22.05	42	42	42	-12.2	-9.71	-2.49	2.49	5.62
hsa-let-7b	F05	33.68	42	42	42	-12.2	-9.71	-2.49	2.49	5.62
hsa-miR-19b	F06	26.09	42	35.72	39.34	-5.92	-7.05	1.13	1.13	2.19
hsa-miR-17	F07	25.68	42	42	42	-12.2	-9.71	-2.49	2.49	5.62
hsa-miR-93	F08	25.5	42	42	42	-12.2	-9.71	-2.49	2.49	5.62
hsa-miR-186	F09	25.87	42	42	42	-12.2	-9.71	-2.49	2.49	5.62
hsa-miR-196b	F10	28.18	42	42	40.48	-12.2	-8.19	-4.01	4.01	16.11
hsa-miR-27a	F11	25.59	42	42	42	-12.2	-9.71	-2.49	2.49	5.62
hsa-miR-22	F12	25.1	42	42	42	-12.2	-9.71	-2.49	2.49	5.62
hsa-miR-130a	G01	25.66	42	42	40.93	-12.2	-8.64	-3.56	3.56	11.79
hsa-let-7c	G02	37.58	42	42	38.61	-12.2	-6.32	-5.88	5.88	58.89
hsa-miR-29c	G03	24.99	42	42	41.92	-12.2	-9.63	-2.57	2.57	5.94
hsa-miR-140-3p	G04	27.11	42	42	36.46	-12.2	-4.17	-8.03	8.03	261.38
hsa-miR-128	G05	25.28	42	42	42	-12.2	-9.71	-2.49	2.49	5.62
hsa-let-7f	G06	Multi Ct	42	42	42	-12.2	-9.71	-2.49	2.49	5.62
hsa-miR-122	G07	32.91	42	42	42	-12.2	-9.71	-2.49	2.49	5.62
hsa-miR-20a	G08	29.23	42	42	42	-12.2	-9.71	-2.49	2.49	5.62
hsa-miR-106b	G09	27.03	42	42	42	-12.2	-9.71	-2.49	2.49	5.62
hsa-miR-7	G10	28	42	42	42	-12.2	-9.71	-2.49	2.49	5.62
hsa-miR-100	G11	22.51	42	42	40.25	-12.2	-7.96	-4.24	4.24	18.90
hsa-miR-302c	G12	42	42	42	42	-12.2	-9.71	-2.49	2.49	5.62
cel-miR-39	H01	42	42	40.83	42	-11.03	-9.71	-1.32	1.32	2.50
cel-miR-39	H02	42	42	42	42	-12.2	-9.71	-2.49	2.49	5.62
SNORD61	H03	28.53	42	42	43.05					
SNORD68	H04	30.08	42	32.74	42.22					
SNORD72	H05	33.51	42	42	42					
SNORD95	H06	23.07	42	15.23	33.13					
SNORD96A	H07	26.7	42	29.8	32.29					
RNU6-2	H08	30.03	42	36.05	42					
miRTC	H09	32.93	34.4	29.28	33.84					
miRTC	H10	33.09	34.32	29.06	30.09					
PPC	H11	23.1	19.58	17.86	22.14					
PPC	H12	18.55	19.68	18.1	21.3					
Avg(h) = C_T(h)		28.65333								

4.8 miRNA DATABASE

The 22 affected miRNAs were searched in miRNA database for their possible target genes and their association with atherosclerosis (see Table 4.3). The tool used for this is available on the site mentioned below.

http://www.exiqon.com/ls/Pages/TPTSequenceInput.aspx?SessionPrefixKey=93e1db75-9df7-452f-8279-c3c96e5cf174

Table 4.3 Predicted target genes and correlation with atherosclerosis of affected miRNAs.

No.	miRNA ID	Target Genes	Disease
1	hsa-miR-142-5p	7	Congestive heart failure [68], Systolic heart failure [69]
2	hsa-miR-150	277	Cardiac hypertrophy [70, 71], Myocardial infarction [72,73]
3	hsa-miR-30c	121	Cardiac hypertrophy [71], Systolic heart failure [69]
4	hsa-miR-96	440	-
5	hsa-miR-185	543	Cardiac hypertrophy [71], Systolic heart failure [69]
6	hsa-miR-142-3p	314	Systolic heart failure [69]
7	hsa-miR-155	251	Acute coronary syndrome [74], Cardiac hypertrophy [71], Congestive heart failure [75], Myocardial infarction [72,73]
8	hsa-miR-425	179	Systolic heart failure [69]
9	hsa-miR-30b	177	Aortic valve stenosis [76], Cardiac hypertrophy [71], Congestive heart failure [77,78], Systolic heart failure [69]
10	hsa-miR-181b	94	Vascular inflammation [79]
11	hsa-miR-320a	115	Congestive heart failure [69], Systolic heart failure [69]
12	hsa-miR-125a-5p	622	Congestive heart failure [78], Systolic heart failure [69]
13	hsa-miR-29a	504	Cardiac hypertrophy [71], Congestive heart failure [78], Inflammation [80], Myocardial infarction [81], Systolic heart failure [69]

Table 4.3 (Cont.)

No.	miRNA ID	Target Genes	Disease
14	hsa-miR-124	391	Systolic heart failure [69]
15	hsa-miR-92a	226	Heart Disease [82,83], Myocardial infarction [84], Systolic heart failure [69]
16	hsa-miR-23a	145	Cardiac hypertrophy [71,85], Congestive heart failure [86,87], Heart disease [88], Systolic heart failure [69], Vascular disease [88,89]
17	hsa-miR-126	56	Atherosclerosis [90,91], Congestive heart failure [78, 92], Heart disease [82,83,84,93] Inflammation [94], Myocardial infarction [95-97], Systolic heart failure [69], Vascular disease [89]
18	hsa-miR-30a	195	Congestive heart failure [78,98], Systolic heart failure [69]
19	hsa-miR-23b	160	Cardiac hypertrophy [71], Congestive heart failure [78], Inflammation [99], Systolic heart failure [69]
20	hsa-miR-151-5p	161	Systolic heart failure [69]
21	hsa-let-7c	358	Cardiac hypertrophy [71], Congestive heart failure [78], Inflammation [100], Systolic heart failure [69]
22	hsa-miR-140-3p	305	Systolic heart failure [69]

CHAPTER 5

DISCUSSION

5.1 MORPHOLOGICAL CHANGES IN HUVECS UNDER FLOW

Vascular endothelial cells are responsible for regulation of variety of physical and biochemical functions of vessel wall. The morphology of endothelial cells plays an important role in maintaining the homeostasis of vascular system. They are continuously being subjected to hemodynamic stimuli *in vivo* like fluid shear stress induced by blood flow [101]. Because of the presence of hemodynamic forces, endothelial cells tend to modify their morphology which in turn causes variation in biochemical function of vascular system by influencing endothelial cells' gene expression. A number of morphological changes were observed in cells by many researchers when the cells were exposed to different flow patterns [102-105]. At the molecular level, hemodynamic forces tend to increase or decrease a variety of genes expression. Atherosclerosis disease progression is strongly related to the stresses endured by vascular cells causing pathology of cardiovascular system [106].

In our experiments, we observed the similar changes in morphology of cells which were consequences of shear stress induced by DMEM flow over HUVECs. The morphological changes during laminar flow experiment showed the elongation of cells in the direction of flow due to alignment of actin filament in response to shear stress. In contrast, disturbed flow experiment portrayed dissimilar results of change in morphology. An unusual variation of spherical cell morphology in disturbed flow region indicated that different flow pattern of flow separation and flow reattachment exerted stimuli on cells from various dimensions. This region involved recirculation eddy currents that is the swirling of fluid over cells when it passed through curvatures

and branched regions. HUVECs under the influence of recirculation eddy were subjected to tangential forces from various dimensions leading to an abrupt change in morphology of cells. This abrupt change in morphology explained the high risk rate of atherosclerosis in branched regions which are more susceptible to disease recurring.

The normal morphology and function of single cell thick endothelial cells is vital for maintaining vascular homeostasis and its dysfunction leads to cardiovascular diseases.

5.2 ANALYSIS OF VARIATION IN GENE EXPRESSION BY REAL TIME PCR

According to one of the previous study on HUVECs exposed to laminar flow for 24 hours with a shear stress of 12.28 dyn/cm^2, 10 miRNAs were found to be significantly affected in their expression [107]. In our study of affect of disturbed flow on miRNA expression in HUVECs, we were expecting the similar variation in expression of miRNAs particularly at branched region of parallel plate flow chamber. In order to verify the change in expression of miRNAs, qPCR analysis was carried out.

PCR is a simple biochemical technique to detect and amplify few copies of a particular DNA sequence across thousands to millions of its copies. This technique is sensitive and specific for DNA amplification. Real time PCR or quantitative PCR (qPCR) was used to quantify cDNA prepared from miRNA, thus determining the gene number in a specific sample. qPCR used fluorescent detection system of SYBR Green that intercalated double stranded DNA and showed fluorescence. qPCR results for the given samples were successful as the housekeeping genes were expressed in every sample. Expression of every gene recorded in the form of Ct was utilized for $\Delta\Delta$Ct analysis. 22 miRNAs were found to be affected in their expression. 9 miRNAs were downregulated and 13 upregulated in the cells exposed to disturbed flow. miRNA database showed the predicted targets of these affected miRNAs and also gave an insight into its relationship with cardiovascular disease focusing on atherosclerosis. hsa-miR-126 is directly involved in regulating atherosclerosis according to database search. This miRNA was downregulated in HUVECs exposed to disturbed flow. This indicated

that at branched region of arteries disturbed flow exerted low shear stress which was sensed by HUVECs resulting in the down regulation of hsa-miR-126. hsa-miR-126 has 56 target genes. VCAM1 (vascular cell adhesion molecule 1) and VEGFA (vascular endothelial growth factor A) being the two targets of hsa-miR-126. The targets of hsa-miR-126 will be up-regulated in response to its own down regulation. Consequently, VCAM1 and VEGFA will be over expressed, resulting in the enhanced recruitment of immune cells at the site of inflammation that causes atherosclerosis progression.

CHAPTER 6

CONCLUSION

In the present study morphological responses of ECs under static condition, laminar flow and disturbed flow conditions were investigated using branched kit parallel plate flow chamber. ECs showed elongation parallel to the direction of flow under laminar flow conditions while in disturbed flow condition, ECs showed spherical morphology. The change in morphology is associated to the abnormal function of ECs that leads to atherosclerosis by variation in expression of several genes.

Gene analysis through qPCR revealed that 22 miRNAs were significantly changed in expression under disturbed flow conditions. 9 miRNAs were down regulated and 13 upregulated. miRNA database showed that down regulated hsa-miR-126 has its direct affect in regulating atherosclerosis. Among its 56 target genes VCAM-1 and VEGFA are two important targets that are directly involved in regulating atherosclerosis.

REFERENCES

[1] Petersen, S., Peto, V., Rayner, M., Leal, J., Luengo-Fernandez, R. and Gray, A., *European Cardiovascular Disease Statistics*, Edition 2005.

[2] Ross R., "Atherosclerosis –An inflammatory disease", *The New England Journal of Medicine*, Vol. 340, pp.115-126, 1999.

[3] Tomkin, G.H. and Owens, D., "LDL as a Cause of Atherosclerosis", *The Open Atherosclerotic & Thrombosis Journal,* Vol. 5, pp. 13-21, 2012.

[4] Sommer, G., "Mechanical Properties of Healthy and Diseased Human Arteries", *Computation in Engineering and Science,* Vol. 7, September 2008.

[5] Rhodin, J.A.G., "Architecture of the Vessel Wall", *Handbook of Physiology, Section 2,* Vol. 2, 1979.

[6] Atherosclerosis an Inflammatory Disease Russell Ross, PhD.

[7] Hulthe, J. and Fagerberg B., "Circulating Oxidized LDL is Associated with Subclinical Atherosclerosis Development and Inflammatory Cytokines (Air Study)", *Arterioscler. Thromb. Vasc. Biol*., Vol. 22, pp. 1162–1167, 2002.

[8] Choi, T., Ahmadi, N., Sourayanezhad, S., Zeb, I. and Budoff, M.J., "Relation of Vascular Stiffness with Epicardial and Pericardial Adipose Tissues, and Coronary Atherosclerosis", *Atherosclerosis,* Vol. 229, pp. 118-123, 2013.

[9] Gotlieb, A.I. and Langille, BL., "The Role of Rheology in Atherosclerotic Coronary Artery Disease", Vol. 1, pp. 595-606, 1996.

[10] Pradhan, S. and Sumpio, B., "Molecular and Biological Effects of Hemodynamics on Vascular Cells", *Bioscience,* Vol. 9, pp. 3276-3285, 2004.

[11] VanderLaan, P.A., Reardon, C.A. and Getz, G.S., "Site Specificity of Atherosclerosis Site-Selective Responses to Atherosclerotic Modulators", *Arterioscler Thromb Vasc Biology*, Vol. 24, pp. 12-22, 2004.

[12] Chiu, J-J. and Chien, S., "Effects of Disturbed Flow on Vascular Endothelium", *Pathophysiological Basis and Clinical Perspectives Physiol,* Vol. 91, pp. 327–387, 2011.

[13] Markl, M., Brendecke, S.M., Simon, J., Barker, A.J., Weiller, C. and Harloff, A., "Co-registeration of the Distribution of Wall Shear Stress and 140 Complex Plaques of the Aorta", *Magnetic Resonance Imaging,* 2013.

[14] Gijsen, F., Giessen. A., Steen, A. and Wentzel, J., "Shear Stress and Advanced Atherosclerosis in Human Coronary Arteries", *Journal of Biomechanics,* Vol. 46, pp. 240-247, 2013.

[15] Chien S., "Mechanotransduction and Endothelial Cell Homeostasis"; *The Wisdom of the Cell,* Vol. 292, pp. 1209–1224, 2007.

[16] Cunningham, K.S. and Gotlieb, A.I., "The Role of Shear Stress in the Pathogenesis of Atherosclerosis", *Lab Invest,* Vol. 85, pp. 9–23, 2005.

[17] Davies, P.F., "Flow-Mediated Endothelial Mechanotransduction", *Physiol Rev,* Vol. 75, pp. 519–560, 1995.

[18] Li, Y.S., Haga, J.H., Chien, S., "Molecular Basis of the Effects of Shear Stress on Vascular Endothelial Cells", *J Biomech,* Vol. 38, pp. 1949–1971, 2005.

[19] Resnick, N., Gimbrone, M.A.Jr., "Hemodynamic Forces are Complex Regulators of Endothelial Gene Expression", *FASEB J,* Vol. 9, pp. 874–882, 1995.

[20] Traub, O., Berk, B.C., "Laminar Shear Stress: Mechanisms by which Endothelial Cells Transduce an Atheroprotective Force", *Arterioscler Thromb Vasc Biol,* Vol. 18, pp. 677–685, 1998.

[21] Bergan, J.J., Schmid-Schönbein, G.W., Smith, P.D., Nicolaides, A.N., Boisseau, M.R., Eklof, B., "Chronic Venous Disease", *N Engl J Med,* Vol. 355, pp. 488–498, 2006.

[22] Chiu, J.J., Usami, S., Chien, S., "Vascular Endothelial Responses to Altered Shear Stress: Pathologic Implications for Atherosclerosis", *Ann Med,* Vol. 41, pp. 19–28, 2009.

[23] Dimmeler, S., Haendeler, J., Zeiher, A.M., "Regulation of Endothelial Cell Apoptosis in Atherothrombosis", *Curr Opin Lipidol,* Vol. 13, pp. 531–536, 2002.

[24] Chiu. J-J., Chien, S., "Effects of Disturbed Flow on Vascular Endothelium: Pathophysiological Basis and Clinical Perspectives", *Physiol Rev,* Vol. 91, pp. 327–387, 2011.

[25] Boisseau, M.R., "Roles of Mechanical Blood Forces in Vascular Diseases", *A Clinical Overview. Clin Hemorheol Microcirc,* Vol. 33, pp. 201–207, 2005.

[26] Gimbrone, M.A.Jr., Resnick, N., Nagel, T., Khachigian, L.M., Collins, T., Topper, J.N., "Hemodynamics, Endothelial Gene Expression, and Atherogenesis", *Ann NY Acad Sci,* Vol. 811, pp. 1–11, 1997.

[27] Malek, A.M., Alper, S.L., Izumo, S., "Hemodynamic Shear Stress and its Role in Atherosclerosis", *JAMA,* Vol. 282, pp. 2035–2042, 1999.

[28] Topper, J.N., Gimbrone, M.A. Jr., "Blood Flow and Vascular Gene Expression: Fluid Shear Stress as a Modulator of Endothelial Phenotype", *Mol Med Today,* Vol. 5, pp. 40–46, 1999.

[29] Asakura, T., Karino, T., "Flow Patterns and Spatial Distribution of Atherosclerotic Lesions in Human Coronary Arteries", *Circ Res,* Vol. 66, pp. 1045–1066, 1990.

[30] Davies, P.F., "Spatial Hemodynamics, the Endothelium, and Focal Atherogenesis: A Cell Cycle Link", *Circ Res,* Vol. 86, pp. 114–116, 2000.

[31] Nerem, R.M., Alexander, R.W., Chappell, D.C., Medford, R.M., Varner, S.E., Taylor, W.R., "The Study of the Influence of Flow on Vascular Endothelial Biology", *Am J Med Sci,* Vol. 316, pp. 169–175, 1998.

[32] Drexler, H., Hornig, B., "Endothelial Dysfunction in Human Disease", *J Mol Cell Cardiol,* Vol. 31, pp. 51–60, 1999.

[33] Azumi, H., Inoue, N., Takeshita, S., Rikitake, Y., Kawashima, S., Hayashi, Y., Itoh, H., Yokoyama, M., "Expression of NADH/NADPH Oxidase p22phox in Human Coronary Arteries", *Circulation,* Vol. 100, pp. 1494–1498, 1999.

[34] Minor, R.L. Jr., Myers, P.R., Guerra, R. Jr., Bates, J.N., Harrison, D.G., "Diet-induced Atherosclerosis Increases the Release of Nitrogen Oxides from Rabbit Aorta", *J Clin Invest,* Vol. 86, pp. 2109–2116, 1990.

[35] Warnholtz, A., Nickenig, G., Schulz, E., Macharzina, R., Brasen, J.H., Skatchkov, M., Heitzer, T., Stasch, J.P., Griendling, K.K., Harrison, D.G., Bohm, M., Meinertz, T., Munzel, T., "Increased NADH-Oxidase Mediated Superoxide Production in the Early Stages of Atherosclerosis: Evidence for Involvement of the Renin-angiotensin System", *Circulation,* Vol. 99, pp. 2027–2033, 1999.

[36] Davies, P.F., Polacek, D.C., Shi, C., Helmke, B.P., "The Convergence of Haemodynamics, Genomics, and Endothelial Structure in Studies of the Focal Origin of Atherosclerosis", *Biorheology,* Vol. 39, pp. 299–306, 2002.

[37] Gimbrone, M.A. Jr., Anderson, K.R., Topper, J.N., Langille, B.L., Clowes, A.W., Bercel, S., Davies, M.G., Stenmark, K.R., Frid, M.G., Weiser-Evans, M.C., Aldashev, A.A., Nemenoff, R.A., Majesky, M.W., Landerholm, T.E., Lu, J., Ito, W.D., Arras, M., Scholz, D., Imhof, B., Aurrand-Lions, M., Schaper, W., Nagel, T.E., Resnick, N., Dewey, C.F., Gimbrone, M.A., Davies, P.F., "The Critical Role of Mechanical Forces in Blood Vessel Development, Physiology and Pathology", *J Vasc Surg,* Vol. 29, pp. 1104–1151, 1999.

[38] Jo, H., Song, H., Mowbray, A., "Role of NADPH Oxidases in Disturbed Flow and BMP4-induced Inflammation and Atherosclerosis", *Antioxid Redox Signal,* Vol. 8, pp. 1609–1619, 2006.

[39] Kamm, R.D., “Cellular Fluid Mechanics”, *Annu Rev Fluid Mech,* Vol. 34, pp. 211–232, 2002.

[40] Giddens, D.P., Zarins, C.K., Glagov, S., "The Role of Fluid Mechanics in the Localization and Detection of Atherosclerosis”, *J Biomech Eng*, Vol. 115, pp. 588–594, 1993.

[41] Buga, G.M., Gold, M.E., Fukuto, J.M., Ignarro, L.J., “Shear Stress Induced Release of Nitric Oxide from Endothelial Cells Grown on Beads”, *Hypertension,* Vol. 17, pp. 187–193, 1991.

[42] Cooke, J.P., “Flow, NO and Atherogenesis”, *Proc Natl Acad Sci USA,* Vol. 100, pp. 768–770, 2003.

[43] McLenachan, J.M., Vita, J., Fish, D.R., Treasure, C.B., Cox, D.A., Ganz, P., Selwyn, A.P., “Early Evidence of Endothelial Vasodilator Dysfunction at Coronary Branch Points”, *Circulation*, Vol. 82, pp. 1169–1173, 1990.

[44] Gambillara, V., Chambaz, C., Roy, S., Stergiopulos, N., Silacci, P., “Plaque-prone Hemodynamics Impairs Endothelial Function in Pig Carotid Arteries”, *Am J Physiol Heart Circ Physiol,* Vol. 290, pp. 2320–2328, 2006.

[45] Duncker, D.J., Bache, R.J., “Regulation of Coronary Blood Flow during Exercise”, *Physiol Rev,* Vol. 88, pp. 1009–1086, 2008.

[46] Cheng, C., Tempel, D., van Haperen, R., van der Baan, A., Grosveld, F., Daemen, M.J., Krams, R., de Crom, R., “Atherosclerotic Lesion Size and Vulnerability are Determined by Patterns of Fluid Shear Stress”, *Circulation,* VoL. 113, pp. 2744–2753, 2006.

[47] Negishi, M., Lu, D., Zhang, Y.Q., Sawada, Y., Sasaki, T., Kayo, T., Ando, J., Izumi, T., Kurabayashi, M., Kojima, I., Masuda, H., Takeuchi, T., “Upregulatory Expression of Furin and Transforming Growth Factor Beta by Fluid Shear Stress in Vascular Endothelial cells”, *Arterioscler Thromb Vascr Biol*, Vol. 21, pp. 785–790, 2001.

[48] Hochleitner, B.W., Hochleitner, E.O., Obrist, P., Eberl, T., Amberger, A., Xu, Q., Margreiter, R., Wick, G., “Fluid Shear Stress Induces Heat Shock Protein 60 Expression in Endothelial Cells in Vitro and in Vivo”, *Arterioscler Thromb Vasc Biol,* Vol. 20, pp. 617–623, 2000.

[49] Ishida, M., Komori, K., Yonemitsu, Y., Taguchi, K., Onohara, T., Sugimachi, K., “Immunohistochemical Phenotypic Alterations of Rabbit Autologous Vein Grafts Implanted under Arterial Circulation with or without Poor Distal Runoff-Implications of Vein Graft Remodeling”, *Atherosclerosis,* Vol. 154, pp. 345–354, 2001.

[50] Hutchison, K.J., “Endothelial Cell Morphology around Graded Stenosis of the Dog Common Carotid Artery”, *Blood Vessels*, Vol. 28, pp. 396–406, 1991.

[51] Levesque, M.J., Liepsch, D., Moravec, S., Nerem, R.M., "Correlation of Endothelial Cell Shape and Wall Shear Stress in a Stenosed Dog Aorta", *Arteriosclerosis*, Vol. 6, pp. 220–229, 1986.

[52] Kim, D.W., Gotlieb, A.I., Langille, B.L., "In Vivo Modulation of Endothelial F-Actin Microfilaments by Experimental Alterations in Shear Stress", *Arteriosclerosis*, Vol. 9, pp. 439–445, 1989.

[53] Porat, R.M., Grunewald, M., Globerman, A., Itin, A., Barshtein, G., Alhonen, L., Alitalo, K., Keshet, E., "Specific Induction of Tie1 Promoter by Disturbed Flow in Atherosclerosis-Prone Vascular Niches and Flow-Obstructing Pathologies", *Circ Res*, Vol. 94, pp. 394–401, 2004.

[54] Walpola, P.L., Gotlieb, A.I., Cybulsky, M.I., Langille, B.L., "Expression of ICAM-1 and VCAM-1 and Monocyte Adherence in Arteries Exposed to Altered Shear Stress", *Arterioscler Thromb Vasc Biol*, Vol. 15, pp. 2–10, 1995.

[55] Zampetaki, A., Zeng, L., Margariti, A., Xiao, Q., Li, H., Zhang, Z., Pepe, A.E., Wang, G., Habi, O., deFalco, E., Cockerill, G., Mason, J.C., Hu, Y., Xu, Q., "Histone Deacetylase 3 is Critical in Endothelial Survival and Atherosclerosis Development in Response to Disturbed flow", *Circulation*, Vol. 121, pp. 132–142, 2010.

[56] Chen, B. P. C., Li, Y.S., Zhao, Y., Chen, K.-D., Li, S., Lao, J., Yuan, S., Shyy, J.Y.J., and Chien, S., "DNA Microarray Analysis of Gene Expression in Endothelial Cells in Response to 24-h Shear Stress", *Physiol Genomics*, Vol.7, pp. 55-63, 2001.

[57] Laughlin, M. H., Newcomer, S.C., and Bender, S.B., "Importance of Hemodynamic Forces as Signals for Exercise-induced changes in Endothelial Cell Phenotype", *Applied Physiology*, Vol. 104, pp. 588-600, 2007.

[58] Pradhan, S., and Sumpio, B., "Molecular and Biological Effects of Hemodynamics on Vascular Cells", *Bioscience*, Vol. 9, pp. 3276-3285, 2004.

[59] VanderLaan, P.A., Reardon, C.A., and Getz, G.S., "Site Specificity of Atherosclerosis Site-Selective Responses to Atherosclerotic Modulators", *Arterioscler Thromb Vasc Biology*, Vol. 24, pp. 12-22, 2004.

[60] Warboys, C.M., Amini, N., Luca, A., and Evans, P.C., "The Role of Blood Flow in Determining the Sites of Atherosclerotic Plaques", *F1000 Medicine Reports*, 2011.

[61] Tarbell, J.M., "Mass Transport in Arteries and the Localization of Atherosclerosis", *Annu. Rev. Biomed. Eng.*, Vol. 5, pp. 79-118, 2003

[62] Qin, X., Wang, X., Wang, Y., Tang, Z., Cui, Q., Xi, J., Li, Y. S. J., Chien, S. and Wang, N., "MicroRNA-19a Mediates the Suppressive Effect of Laminar Flow on Cyclin D1Expression in Human Umbilical Vein Endothelial Cells", *PNAS*, Vol. 107, pp. 3240-3244, 2010.

[63] George, S., "On the Effect of the Internal friction of Fluids on the Motion of Pendulums", *Transactions of the Cambridge Philosophical Society,* Vol. 9, pp. 8-106, 1851.

[64] Chomczynski, P., *Bio Techniques* Vol. 15, pp. 532-537, 1993.

[65] Chomczynski, P. & Sacchi, N., *Anal Biochem,* Vol. 162**,** 156-159, 1987.

[66] miScript™ miRNA PCR Array Handbook, October 2011.

[67] Goni, R. Garcia, P. & Foissac, S., "The qPCR Data Statistical Analysis" *Integromics White Paper*, September 2009.

[68] Voellenkle C., Van Rooij J., Cappuzzello C., Greco S., Arcelli D., Di Vito L., Melillo G., Rigolini R., Costa E., Crea F., Capogrossi MC., Napolitano M. & Martelli F., "Micro RNA Signatures in Peripheral Blood Mononuclear Cells of Chronic Heart Failure Patients", *Physiol Genomics,* Vol. 42, pp. 420-6, Aug. 2010.

[69] Goren Y., Kushnir M., Zafrir B., Tabak S., Lewis BS. & Amir O., "Serum Levels of MicroRNAs in Patients with Heart Failure", *Eur J Heart Fail,* Vol. 12, pp. 147-54, Feb. 2012.

[70] Cheng Y., Ji R., Yue J., Yang J., Liu X., Chen H., Dean DB. & Zhang C., "MicroRNAs are Aberrantly Expressed in Hypertrophic Heart: Do They Play a Role in Cardiac Hypertrophy?", *Am J Pathol*, Vol. 170, pp. 1831-40, Jun 2007.

[71] Sayed D., Hong C., Chen IY., Lypowy J. & Abdellatif M., "MicroRNAs Play an Essential Role in the Development of Cardiac Hypertrophy", *Circ Res*, Vol. 100, pp. 416-24, Feb. 2007.

[72] Zidar N., Boštjančič E., Glavač D. & Stajer D., "MicroRNAs, Innate Immunity and Ventricular Rupture in Human Myocardial Infarction", *Dis Markers*, Vol. 31, pp. 259-65, 2011.

[73] Bostjancic E., Zidar N. & Glavac D., "microRNA Microarray Expression Profiling in Human Myocardial Infarction", *Dis Markers*, Vol. 27, pp.255-68, 2009.

[74] Yao R., Ma Y., Du Y., Liao M., Li H., Liang W., Yuan J., Ma Z., Yu X., Xiao H. & Liao Y., "The Altered Expression of Inflammation-Related MicroRNAs with Microrna-155 Expression Correlates with Th17 Differentiation in Patients with Acute Coronary Syndrome", *Cell Mol Immunol*, Vol. 8, pp. 486-95, Nov. 2011.

[75] Blanco R. R., Austin H., Vest R. N. 3rd, Valadri R., Li W., Lassegue B., Song Q., London B., Dudley S. C., Bloom H. L., Searles C. D. & Zafari A. M., "Angiotensin Receptor Type 1 Single Nucleotide Polymorphism 1166a/C is Associated with Malignant Arrhythmias and Altered Circulating Mir-155 Levels in Patients with Chronic Heart Failure", *J Card Fail*, Vol. 18, pp. 717-23, Sep. 2012.

[76] Nigam V., Sievers H. H., Jensen B. C., Sier H. A., Simpson P. C., Srivastava D. & Mohamed S. A., "Altered MicroRNAs in Bicuspid Aortic Valve: A Comparison between Stenotic and Insufficient Valves", *J Heart Valve Dis* Vol. 19, pp. 459-65, Jul. 2010.

[77] Duisters R. F., Tijsen A. J., Schroen B., Leenders J. J., Lentink V., Van der Made I., Herias V., Van Leeuwen R. E., Schellings M. W., Barenbrug P., Maessen J. G., Heymans S. & Pinto Y. M., Creemers E. E., "miR-133 and mir-30 Regulate Connective Tissue Growth Factor: Implications for a Role of MicroRNAs in Myocardial Matrix Remodeling", *Circ Res*, Vol. 104, pp. 170-8, Jan. 2009.

[78] Thum T., Galuppo P., Wolf C., Fiedler J., Kneitz S., Van Laake L. W., Doevendans P. A., Mummery C. L., Borlak J., Haverich A., Gross C., Engelhardt S., Ertl G. & Bauersachs J., "MicroRNAs in the Human Heart: A Clue to Fetal Gene Reprogramming in Heart Failure", *Circulation*, Vol. 116, pp. 258-67, Jul. 2007.

[79] Sun X., Icli B., Wara A. K., Belkin N., He S., Kobzik L., Hunninghake G. M., Vera M. P.; MICU Registry, Blackwell T. S., Baron R. M. & Feinberg M. W., "Microrna-181b Regulates Nf-Kb-Mediated Vascular Inflammation", *J Clin Invest*, Vol. 122, pp. 1973-90, Jun. 2012.

[80] Chen T., Li Z, Tu J., Zhu W., Ge J., Zheng X., Yang L., Pan X., Yan H. & Zhu J., "Microrna-29a Regulates Pro-Inflammatory Cytokine Secretion and Scavenger Receptor Expression by Targeting Lpl In Oxldl-Stimulated Dendritic Cells", *Circulation*, Vol. 585, pp. 657-63, Feb. 2011.

[81] Zile M. R., Mehurg S. M., Arroyo J. E., Stroud R. E., DeSantis S. M. & Spinale F. G., "Relationship between the Temporal Profile of Plasma MicroRNA and Left Ventricular Remodeling in Patients After Myocardial Infarction", *Circ Cardiovasc Genet*, Vol. 4, pp. 614-9, Dec. 2011.

[82] Zhang Q., Kandic I. & Kutryk M. J., "Dysregulation of Angiogenesis-Related Micrornas in Endothelial Progenitor Cells from Patients with Coronary Artery Disease", *Biochem Biophys Res Commun*, Vol. 405, pp. 42-6, Feb. 2011.

[83] Fichtlscherer S., De Rosa S., Fox H., Schwietz T., Fischer A., Liebetrau C., Weber M., Hamm C. W., Röxe T., Müller-Ardogan M., Bonauer A., Zeiher A. M. & Dimmeler S., "Circulating Micrornas in Patients with Coronary Artery Disease", *Circ Res*, Vol. 107, pp. 677-84, Sep. 2010.

[84] Wang H., Lin Y. Z., Lu H. M., Zhou Y., Luo C., Lu S. H., Zhao L. & Liu F., "Circulating Microrna-92a in Patients with St-Segment Elevation Myocardial Infarction", *Zhongguo Wei Zhong Bing Ji Jiu Yi Xue*, Vol. 23, pp. 18-22, Dec. 2011.

[85] Lin Z., Murtaza I., Wang K., Jiao J., Gao J. & Li P. F., "Mir-23a Functions Downstream of Nfatc3 To Regulate Cardiac Hypertrophy", *Proc Natl Acad Sci U S A*, Vol. 106, pp. 12103-8, Jul. 2009.

[86] Ramani R., Vela D., Segura A., McNamara D., Lemster B., Samarendra V., Kormos R., Toyoda Y., Bermudez C., Frazier O. H., Moravec C. S., Gorcsan J. 3rd, Taegtmeyer H. & McTiernan C. F., "A Micro-Ribonucleic Acid Signature Associated with Recovery from Assist Device Support in 2 Groups of Patients with Severe Heart Failure", *J Am Coll Cardiol*, Vol. 58, pp. 2270-8, Nov. 2011.

[87] Van Rooij E., Sutherland L. B., Liu N., Williams A. H., McAnally J., Gerard R. D., Richardson J. A. & Olson E. N., "A Signature Pattern of Stress-Responsive MicroRNAs that can Evoke Cardiac Hypertrophy and Heart Failure", *Proc Natl Acad Sci U S A*, Vol. 103, pp. 18255-60, Nov. 2006.

[88] Bang C., Fiedler J. & Thum T., "Cardiovascular Importance of the Microrna-23/27/24 Family", *Microcirculation*, Vol. 19, pp. 208-14, Apr. 2012.

[89] Larsson E., Fredlund Fuchs P., Heldin J., Barkefors I., Bondjers C., Genové G., Arrondel C., Gerwins P., Kurschat C., Schermer B., Benzing T., Harvey S. J., Kreuger J. & Lindahl P., "Discovery of Microvascular Mirnas using Public Gene Expression Data: Mir-145 is Expressed in Pericytes and is a Regulator of Fli1", *Genome Med*, Vol. 1, pp. 108, Nov. 2009.

[90] Dentelli P., Rosso A., Orso F., Olgasi C., Taverna D. & Brizzi M. F., "Microrna-222 Controls Neovascularization by Regulating Signal Transducer and Activator of Transcription 5a Expression", *Arterioscler Thromb Vasc Biol*, Vol. 30, pp. 1562-8, Aug. 2010.

[91] Zernecke A., Bidzhekov K., Noels H., Shagdarsuren E., Gan L., Denecke B., Hristov M., Köppel T., Jahantigh M. N., Lutgens E., Wang S., Olson E. N., Schober A. & Weber C., "Delivery of Microrna-126 by Apoptotic Bodies Induces Cxcl12-Dependent Vascular Protection", *Sci Signal*, Vol. 2, Dec. 2009.

[92] Fukushima Y., Nakanishi M., Nonogi H., Goto Y. & Iwai N., "Assessment of Plasma miRNAs in Congestive Heart Failure", *Circ J*, Vol. 75, pp. 336-40, 2011.

[93] De Rosa S., Fichtlscherer S., Lehmann R., Assmus B., Dimmeler S. & Zeiher A.M., "Trans Coronary Concentration Gradients of Circulating MicroRNAs", *Circulation*, Vol. 124, pp. 1936-44, Nov. 2011.

[94] Asgeirsdóttir S. A, Van Solingen C., Kurniati N. F., Zwiers P. J., Heeringa P., Van Meurs M., Satchell S. C., Saleem M. A., Mathieson P. W., Banas B., Kamps J. A., Rabelink T. J.,Van Zonneveld A. J. & Molema G., "MicroRNA-126 Contributes to Renal Microvascular Heterogeneity of VCAM-1 Protein Expression in Acute Inflammation", *Am J Physiol Renal Physiol*, Vol. 302, pp. 1630-9, Jun. 2012.

[95] Long G., Wang F., Duan Q., Chen F., Yang S., Gong W., Wang Y., Chen C. & Wang D. W., "Human Circulating microRNA-1 and microRNA-126 as Potential Novel Indicators for Acute Myocardial Infarction", Int J Biol Sci, Vol. 8, pp. 811-8, 2012.

[96] Zampetaki A., Willeit P., Tilling L., Drozdov I., Prokopi M., Renard J. M., Mayr A., Weger S., Schett G., Shah A., Boulanger C. M., Willeit J., Chowienczyk P.

J., Kiechl S. & Mayr M., "Prospective Study on Circulating MicroRNAs and Risk of Myocardial Infarction", *J Am Coll Cardiol,* Vol. 60, pp. 290-9, Jul. 2012.

[97] Shi B., Guo Y., Wang J. & Gao W., "Altered Expression of microRNAs in the Myocardium of Rats with Acute Myocardial Infarction", *BMC Cardiovasc Disord,* Vol. 10, Mar. 2010.

[98] Duisters R. F., Tijsen A. J., Schroen B., Leenders J. J., Lentink V., Van der Made I., Herias V., Van Leeuwen R. E., Schellings M. W., Barenbrug P., Maessen J. G., Heymans S.,Pinto Y. M. & Creemers E. E., "miR-133 and miR-30 Regulate Connective Tissue Growth Factor: Implications for a Role of microRNAs in Myocardial Matrix Remodeling", Circ Res, Vol. 104, pp. 170-8, Jan 2009.

[99] Zhu S., Pan W., Song X., Liu Y., Shao X., Tang Y., Liang D., He D., Wang H., Liu W., Shi Y., Harley J. B., Shen N. & Qian Y., "The microRNA miR-23b Suppresses IL-17-associated Autoimmune Inflammation by Targeting TAB2, TAB3 and IKK-α", *Circulation*, Vol. 18, pp. 1077-86, Jul. 2012.

[100] Kumar M., Ahmad T., Sharma A., Mabalirajan U., Kulshreshtha A., Agrawal A. & Ghosh B., "Let-7 microRNA-mediated Regulation of IL-13 and Allergic Airway Inflammation", *J Allergy Clin Immunol*, Vol. 128, pp. 1077-85, Nov. 2011.

[101] Kudo, S., Yamaguchi, R., Ikeda, M. and Tanishita, K., "Effect of Fluid Force on Vascular Cell Function", *Physiol. Anthropol. Appl. Human Sei*, Vol. 24, pp. 459-461, 2005.

[102] Kwak, B.R., Mulhaupt, F., Veillard, N., Gros, D.B. and Mach, F., "Altered Pattern of Vascular Connexin Expression in Atherosclerotic Plaques*", Arterioscler. Thromb. Vasc. Biol.,* Vol. 22, pp. 225–230, 2002.

[103] Arslan, N., Işık, S. and Uykan, Ö., "Steady and Disturbed Flow Effects on Human Umbilical Vein Endothelial Cells (HUVECs) in Vascular System: an Experimental Study*", Acta of Bioengineering and Biomechanics*, Vol. 12, pp. 3-9, 2010.

[104] Miao, H., Hu, Y.L., Shiu, Y.T., Yuan, S., Zhao, Y., Kaunas, R., Wang, Y., Jin, G., Usami, S.and Chien, S., "Effects of Flow Patterns on the Localization and Expression of VE cadherin at Vascular Endothelial Cell Junctions: in vivo and in vitro Investigations", *JVasc.Res.*, Vol. 42, pp. 77-89, 2005.

[105] Chatzizisis, Y. S., Coskun, A. U.,Jonas, M., Edelman, E.R., Feldman, C.L. and Stone, P.H., ""Role of Endothelial Shear Stress in the Natural History of Coronary Atherosclerosis and Vascular Remodeling Molecular, Cellular, and Vascular Behavior", *JACC,* Vol. 49, pp. 2379-2393, 2007.

[106] Resnick, N., Yahav, H., Salita, S., Shushy, Y., Schubert, S., Zilberman, L.C.M. and Wofovitz, E.," Fluid Shear Stress and the Vascular Endothelium: for Better and for Worse", *Progress in Biophysics & Molecular Biology*, Vol. 81, pp. 177-199, 2003.

[107] Özbal, H.K., *Quantitative Real Time PCR Array Analysis of miRNA in Endothelial Cells Exposed to Laminar and Disturbed Flow Conditions*, M.S. Thesis, Fatih University, 2012.